INTERNATIONAL JOURNAL FOR NUMERICAL METHODS IN FLUIDS
Int. J. Numer. Meth. Fluids **28**: 157–186 (1998)

A SEMI-IMPLICIT METHOD FOR VERTICAL TRANSPORT IN MULTIDIMENSIONAL MODELS

EDWARD S. GROSS[a], VINCENZO CASULLI[b,c], LUCA BONAVENTURA[b,c] AND JEFFREY R. KOSEFF[a]

[a] *Environmental Fluid Mechanics Laboratory, Department of Civil and Environmental Engineering, Stanford University, Stanford, CA 94305-4020, USA*
[b] *Dipartimento di Ingegneria Civile ed Ambientale, Università di Trento, Mesiano di Povo, 38050 (TN), Italy*
[c] *CIRM-ITC, Povo, 88050 (TN), Italy*

SUMMARY

A one-dimensional scalar transport method which is appropriate for simulations over a wide range of Courant number is described. Von Neumann stability and matrix invertibility are guaranteed for all Courant numbers and the method has less diffusive and dispersive error than simpler implicit methods. It is implemented for vertical scalar transport in a three-dimensional hydrodynamic model, with horizontal transport discretized explicitly. The method is applied and compared with simpler semi-implicit methods in several test cases and used for a simulation of scalar transport in an estuary. © 1998 John Wiley & Sons, Ltd.

KEY WORDS: advective transport; semi-implicit; conservative; unconditionally stable

1. INTRODUCTION

The focus of this paper is on the numerical solution of the scalar transport equation in conservative form

$$\frac{\partial s}{\partial t}+\frac{\partial (us)}{\partial x}+\frac{\partial (vs)}{\partial y}+\frac{\partial (ws)}{\partial z}=\frac{\partial}{\partial x}\left(\epsilon_{\mathrm{h}}\frac{\partial s}{\partial x}\right)+\frac{\partial}{\partial y}\left(\epsilon_{\mathrm{h}}\frac{\partial s}{\partial y}\right)+\frac{\partial}{\partial z}\left(\epsilon_{\mathrm{v}}\frac{\partial s}{\partial z}\right), \tag{1}$$

where $s(x, y, z, t)$ is the scalar concentration, $\epsilon_{\mathrm{h}}(x, y, z, t)$ is the horizontal diffusion coefficient, $\epsilon_{\mathrm{v}}(x, y, z, t)$ is the vertical diffusion coefficient and $u(x, y, z, t)$, $v(x, y, z, t)$, $w(x, y, z, t)$ are the velocity components in the horizontal x-, y-directions and vertical z-direction, respectively. Given that u, v and w are calculated by a hydrodynamic model, and that appropriate values of ϵ_{h} and ϵ_{v} are supplied by a turbulence closure model, a method to solve Equation (1) will be outlined in this paper. The conservative method outlined will be incorporated into the tidal, residual, intertidal mudflat three-dimensional (TRIM-3D) [1] model as an alternative to the non-conservative Eulerian–Lagrangian method [2].

Special attention is given to the vertical advective transport terms, because the grid spacing chosen in the vertical is generally much smaller than the horizontal grid spacing in estuarine and ocean modeling. When a fixed level grid is used, as in the implementation reported here, the grid spacing of the top and bottom cells can be very small, even approaching zero as the top cells become wet and dry. Therefore, if vertical advection were treated explicitly in time, a strict stability condition would result. In addition, since one of the main goals of such models

CCC 0271–2091/98/110157–30$17.50
© 1998 John Wiley & Sons, Ltd.
Received January 1997
Revised August 1997

is the study of vertical mixing, a scheme with low numerical diffusion must be devised for vertical advection.

The present method is designed to be used in cases with a wide range of Courant numbers, such that Courant numbers for most computational cells are small, and the location and time at which high Courant numbers arise can not be predicted *a priori*. These conditions are very common for transport modeling in estuaries. For example, in South San Francisco Bay (SSFB), relatively low vertical velocities are present in most of the estuary throughout the tidal cycle, but higher velocities can occur in regions with sharp bathymetry gradients or strong baroclinic motions. In Figure 1 we plot the frequency of vertical velocity magnitude used for transport calculations in SSFB during one tidal cycle. While over 98% of the vertical velocities are lower than 0.2 cm s^{-1}, the highest vertical velocity experienced in this period was 2.1 cm s^{-1}. Thus, a method that is highly accurate for low Courant numbers (e.g. $|c_z| < 1$) is desired and some accuracy at high Courant numbers may be sacrificed in order to avoid imposing an excessive limitation on the time step.

Clearly, an implicit or semi-implicit method is required for this purpose. Two commonly used implicit methods are implicit upwind and central differencing. Implicit upwind differencing, which uses backward Euler time advancement and first-order upwind spatial differencing, is highly diffusive for practical grid spacing, while central differencing yields large oscillations. Often, in order to control these oscillations, diffusive filters or large diffusion coefficients are employed. Therefore, the resulting schemes are not well suited for simulations of vertical mixing in estuaries, because high numerical diffusion can obscure the physical mixing and may even exceed the diffusion calculated by the turbulence model. Instead, a scheme with low numerical diffusion, minimal oscillations, a simple matrix structure, and stability for a large range of Courant numbers is required.

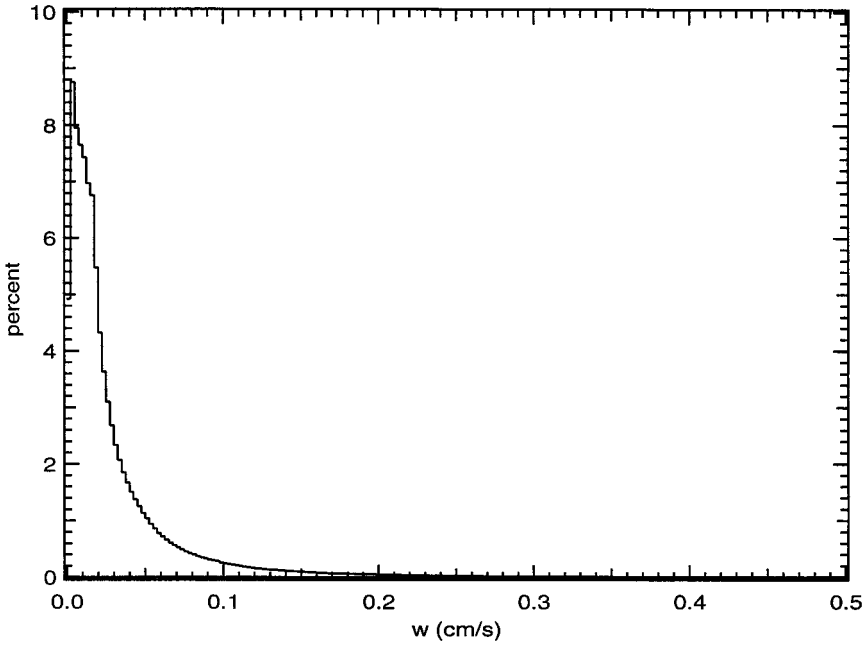

Figure 1. Histogram of magnitude of vertical velocity in South San Francisco Bay. Velocities were calculated using the TRIM-3D [1] model.

© 1998 John Wiley & Sons, Ltd.

To achieve these goals the 'trapezoidal method' in time is used [3], with a combination of the QUICK [4] scheme and first-order upwind differencing in space. A weighting coefficient between QUICK and first-order upwind differencing is chosen to provide minimal numerical diffusion, while still satisfying a von Neumann stability condition and matrix invertibility. At low Courant numbers ($|c_z| < 1$) a combination of the trapezoidal method and QUICK, which we will refer to as QUICKtm, is used. At high Courant numbers ($|c_z| > 1$) the minimal fraction of first-order upwind interpolation, as a function of local $|c_z|$, which allows von Neumann stability is added.

The proposed method is outlined in three parts. First, the vertical advection scheme is presented and analyzed as a one-dimensional method. Next, the vertical diffusion term is taken into account. Then the implicit method for the vertical advection and diffusion terms is used with explicit treatment of the horizontal advection and diffusion terms to model three-dimensional scalar transport.

2. INTRODUCTION OF THE NUMERICAL METHOD

For much of the following discussion the conservative one-dimensional advective transport equation will be considered;

$$\frac{\partial s}{\partial t} + \frac{\partial (ws)}{\partial z} = 0, \tag{2}$$

where s is the transported scalar concentration and w is a velocity. Assuming constant velocity w, we arrive at the equation

$$\frac{\partial s}{\partial t} + w \frac{\partial s}{\partial z} = 0. \tag{3}$$

A finite difference approximation of Equation (3) for constant grid spacing, Δz, can be written as

$$s_k^{n+1} = s_k^n - c_z(s_\mathrm{u} - s_\mathrm{l}), \tag{4}$$

where $c_z = w\Delta t/\Delta z$ is the constant Courant number, Δt is the time step and s_l and s_u are the concentrations at the flux faces, $k - 1/2$ and $k + 1/2$, respectively. The time levels of s_u and s_l are intentionally not specified.

Using this notation, transport schemes are simply methods to interpolate concentration values onto the flux faces of the staggered grid. Since $(s_\mathrm{l})_k = (s_\mathrm{u})_{k-1}$ it suffices to specify the interpolation formula for s_u. Assuming a positive velocity, first-order upwind differencing results in

$$s_\mathrm{u} = s_k, \tag{5}$$

and central differencing gives

$$s_\mathrm{u} = \frac{1}{2}(s_k + s_{k+1}). \tag{6}$$

One alternative used to avoid the shortcomings of first-order upwind differencing and central differencing is the QUICK scheme [4]. Assuming a positive velocity, the interpolation formula is

© 1998 John Wiley & Sons, Ltd.

$$s_u = \frac{1}{2}(s_k + s_{k+1}) - \frac{1}{8}(s_{k-1} - 2s_k + s_{k+1}). \tag{7}$$

The QUICK scheme has a greater accuracy and is less prone to oscillations than central differencing. As originally published, it is explicit and not stable for pure advection.

This scheme can be generalized to 'generalized trapezoidal' time advancement [3] using a variable implicitness parameter $\theta \in (0, 1)$, so that

$$s_u = \frac{\theta}{2}(s_k^{n+1} + s_{k+1}^{n+1}) + \frac{(1-\theta)}{2}(s_k^n + s_{k+1}^n) - \frac{1}{8}(s_{k-1}^n - 2s_k^n + s_{k+1}^n). \tag{8}$$

Note that the term $\frac{1}{8}(s_{k-1}^n - 2s_k^n + s_{k+1}^n)$ is explicit, in order to maintain a tridiagonal matrix structure. Equation (8) with $\theta = 0.5$ will be referred to as QUICKtm. It will be shown that QUICKtm is stable and second-order accurate in time for $|c_z| \leq 1$. In order to maintain stability for higher $|c_z|$, a limited amount of first-order upwind differencing is added, depending on the Courant number itself, as follows:

$$\begin{aligned} s_u = {} & \beta[\theta s_k^{n+1} + (1-\theta)s_k^n] \\ & + (1-\beta)\left[\frac{\theta}{2}(s_k^{n+1} + s_{k+1}^{n+1}) + \frac{(1-\theta)}{2}(s_k^n + s_{k+1}^n) - \frac{1}{8}(s_{k-1}^n - 2s_k^n + s_{k+1}^n)\right], \end{aligned} \tag{9}$$

where the weighting parameter $\beta(c_z) \in (0, 1)$ will be given later. Substituting Equation (9) into (4) results in

$$\begin{aligned} & s_k^{n+1} + \theta c_z\left[\beta(s_k^{n+1} - s_{k-1}^{n+1}) + \frac{1}{2}(1-\beta)(s_{k+1}^{n+1} - s_{k-1}^{n+1})\right] \\ & = s_k^n - (1-\theta)c_z\left[\beta(s_k^n - s_{k-1}^n) + \frac{1}{2}(1-\beta)(s_{k+1}^n - s_{k-1}^n)\right] \\ & \quad - \frac{1}{8}(1-\beta)c_z(s_{k-2}^n - 3s_{k-1}^n + 3s_k^n - s_{k+1}^n). \end{aligned} \tag{10}$$

Equation (10) defines 'the β method' in the case of a constant positive velocity and constant grid spacing. For $\theta = 1$ this method is backward Euler in time and for $\theta = 0.5$ the result is the trapezoidal method for the upwind and central difference terms, while the higher order correction of QUICKtm is explicit. $\beta = 0$ results in QUICKtm, whereas $\beta = 1$ results in first-order upwind differencing. In actual simulations, however, the velocity varies spatially and temporally: β will be chosen accordingly, so that accuracy will be sacrificed only in the limited regions of high Courant number.

In recent years, several approaches which combine the monotonicity preservation property of first-order upwind differencing with higher Taylor series accuracy have been published (see Reference [5] for a review). These approaches, some of which are known as 'total variation diminishing', or TVD methods, essentially involve weighting a high-order scheme (usually second-order) which allows oscillations (such as Lax–Wendroff) with first-order upwind differencing such that the monotonicity of the solution is preserved while the accuracy of the high-order method is retained in regions of smooth scalar gradients [6]. A TVD method which was applied successfully by James [7] in a three-dimensional shelf-sea model, showed large advantages in terms of reduced numerical diffusion relative to first-order upwind differencing while yielding an oscillation-free solution. Explicit TVD methods, however, have a Courant number limitation: usually $c_z \leq 1$. Implicit TVD methods have also been developed but are less common. Yee [8] presented a family of second-order implicit TVD schemes and found that for

© 1998 John Wiley & Sons, Ltd.

a second-order time accurate scheme (using the trapezoidal method) the method is TVD only when $c_z \leq 4/3$. Thus, it appears that second-order time accuracy, which we have shown to be important at high Courant number, and monotonicity preservation, cannot both be ensured for computations at high Courant number. The method presented in this text allows oscillations to occur but retains second-order time accuracy and stability for all c_z.

2.1. Numerical diffusion

The evaluation of eddy diffusivity, a topic of great interest in estuarine physics (see Reference [9]), and complex turbulence models are often applied to model mixing [10]. However, the actual vertical mixing that a numerical model predicts also depends on the numerical diffusion present in the vertical advection scheme. Thus, the numerical diffusion of an advection scheme should be at least one order of magnitude lower than the physical diffusion calculated by the turbulence model. In order to analyze numerical diffusion of discretization schemes, Taylor series expansion is applied to schemes which solve Equation (3). The coefficient of s_{zz} will be referred to as the 'numerical diffusion coefficient'. In addition, the word 'diffusion' in this paper will refer solely to Laplacian diffusion ($\epsilon_{\text{num}} s_{xx}$) and not higher order, biharmonic diffusion ($\epsilon_{\text{bi}} s_{xxxx}$). Not only does first-order upwind result in significant numerical diffusion, but so do typical implementations of leapfrog-central methods due to the use of diffusive filters [10]. In contrast, the method developed here does not add vertical diffusion globally and yields results with weaker oscillations than leapfrog-central.

The general expression for the numerical diffusion coefficient of the β method is:

$$\epsilon_{\text{num}} = \frac{(\Delta z)^2}{\Delta t} |c_z| \left[\left(\theta - \frac{1}{2} \right) |c_z| + \frac{\beta}{2} \right]. \tag{11}$$

This expression consists of the time discretization error

$$\frac{(\Delta z)^2}{\Delta t} c_z^2 \left(\theta - \frac{1}{2} \right), \tag{12}$$

and the space discretization error

$$\frac{(\Delta z)^2}{\Delta t} |c_z| \frac{\beta}{2}. \tag{13}$$

The maximum numerical diffusion coefficient for spatial error results from $\beta = 1$, which represents the diffusive error of the 'trapezoidal upwind' method which uses the trapezoidal method for time integration and first-order upwind for spatial differencing. The maximum numerical diffusion coefficient of temporal error results for $\theta = 1$, which represents the diffusive error associated with backward Euler time advancement. It is clear from Equation (11) that when $\theta = 0.5$ and $\beta = 0$ the numerical diffusion coefficient is zero. Choosing $\theta = 0.5$ and $\beta = 0$ results in the highest accuracy for the β method, thus they will be chosen for the range of $|c_z|$ which satisfies the von Neumann stability condition shown next. For other valid values of θ and β, the time error grows as c_z^2 whereas the spatial error grows as $|c_z|$. Therefore, we prefer to sacrifice spatial accuracy instead of temporal accuracy for high Courant number calculations.

2.2. Stability analysis

Since low numerical diffusion is one of the primary objectives of the proposed method, we will choose $\theta = 0.5$ and $\beta = 0$ as long as stability is guaranteed. For these values of θ and β,

© 1998 John Wiley & Sons, Ltd.

$c_z \leq 1$ is a sufficient condition for stability. Next the method with which to select β as a function of Courant number in order to have stability for $c_z \geq 1$ is shown. A constant positive velocity is used in the analysis, and the stability condition derived for $\theta = 0.5$ is also sufficient for $\theta > 0.5$.

For $\theta = 0.5$ the one-dimensional finite difference Equation (10) reduces to

$$\begin{aligned} & s_k^{n+1} + \frac{1}{2}\, c_z \left[\beta(s_k^{n+1} - s_{k-1}^{n+1}) + \frac{1}{2}(1-\beta)(s_{k+1}^{n+1} - s_{k-1}^{n+1}) \right] \\ & = s_k^n - \frac{1}{2} c_z \left[\beta(s_k^n - s_{k-1}^n) + \frac{1}{2}(1-\beta)(s_{k+1}^n - s_{k-1}^n) \right] \\ & \quad - \frac{1}{8}(1-\beta) c_z (s_{k-2}^n - 3s_{k-1}^n + 3s_k^n - s_{k+1}^n). \end{aligned} \tag{14}$$

The resulting amplification factor is

$$G = \frac{[1 - c_z/2(\beta(1-\cos\alpha) + I\sin\alpha) - \frac{1}{4}(1-\beta)c_z((1-\cos\alpha)^2 + I\sin\alpha(1-\cos\alpha))]}{[1 + c_z/2(\beta(1-\cos\alpha) + I\sin\alpha)]} \tag{15}$$

where α is the phase angle and $I = \sqrt{-1}$ is the imaginary unit. After simplification, the necessary and sufficient condition for stability in the von Neumann sense is reached

$$-2\beta + \frac{1}{8}(1-\beta)(1-\cos\alpha)[-4 + c_z(1-\cos\alpha)(1+\beta) + 2c_z(1+\cos\alpha)] \leq 0. \tag{16}$$

Substitution of $\beta = 0$ into Equation (16) readily yields the condition $c_z \leq 1$. Since unconditional stability is desired, accuracy must be sacrificed for $c_z > 1$. Therefore, it is shown that the choice of

$$\beta(c_z) = \frac{(c_z - 1)^2}{4c_z} \quad \text{for } c_z \geq 1 \tag{17}$$

satisfies inequality (16). Upon substitution of Equation (17) into (16) and simplification, the result is

$$[((c_z - 1)^2 - 4c_z)(1 - \cos\alpha) + 8(c_z - 1)]^2 \geq 0. \tag{18}$$

This condition is always satisfied, thus Equation (17) is sufficient for stability. In addition, if

$$(1 - \cos\alpha) = \frac{-8(c_z - 1)}{(c_z - 1)^2 - 4c_z} \quad \text{for } 1 \leq c_z \leq 3, \tag{19}$$

then inequality (18) is satisfied with the equal sign. For $c_z > 3$ the value of $\cos\alpha$ given by Equation (19) is outside the range $(-1, 1)$. Thus, although Equation (17) is sufficient for stability, it results in higher β values than necessary for von Neumann stability. For $c_z > 3$, the highest amplification factor results from $\cos\alpha = -1$. Substituting $\cos\alpha = -1$ into inequality (16) yields the condition

$$\beta(c_z) = \frac{c_z - 2}{c_z} \quad \text{for } c_z \geq 3, \tag{20}$$

which specifies a smaller value of β in this range than in the previous sufficient condition, (17).

Summarizing, and including results for a negative velocity, the condition of stability of the β method are met if β is given by the following function of $|c_z|$,

© 1998 John Wiley & Sons, Ltd.

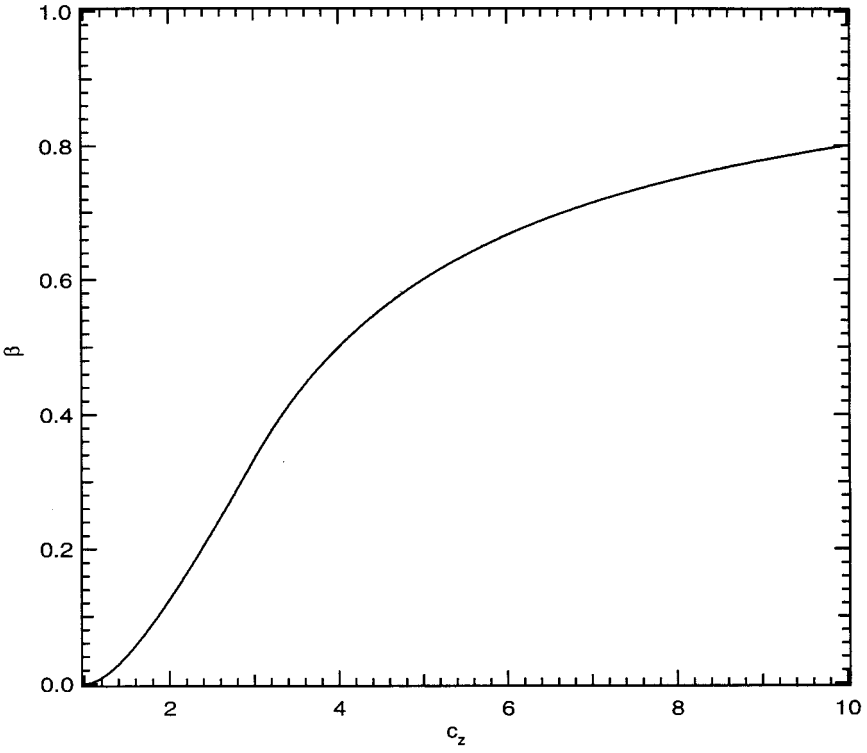

Figure 2. The minimum $\beta = f(c_z)$ which allows stability in the von Neumann sense.

$$\beta(c_z) = \begin{cases} 0 & |c_z| \le 1 \\ \dfrac{(|c_z|-1)^2}{4|c_z|} & 1 \le |c_z| \le 3 \\ \dfrac{|c_z|-2}{|c_z|} & |c_z| \ge 3 \end{cases} \tag{21}$$

which increases monotonically and continuously from 0 to 1. For a value of β lower than that specified by these relations, it is not difficult to find values of α that result in an amplification factor greater than 1. Thus, these conditions are both necessary and sufficient for stability in the von Neumann sense.

The dependence of β on Courant number is plotted in Figure 2. The resulting numerical diffusion (ϵ_{num}) of this method is non-dimensionalized by $(\Delta z)^2/\Delta t$, plotted, and compared with backward Euler upwind differencing and trapezoidal upwind differencing in Figure 3. This figure illustrates that the β method has no numerical diffusion for $|c_z| < 1$ and that numerical diffusion increases quite slowly for $|c_z| < 2$. The diffusive error of trapezoidal upwind differencing is much lower than that of backward Euler upwind differencing for $|c_z| > 1$, illustrating that time accuracy is important at high Courant numbers. Trapezoidal central differencing is free from diffusive error but does have phase error.

The phase error, ε_ϕ, of the β method, trapezoidal upwind differencing and trapezoidal central differencing, is plotted in Figure 4. It is always lagging phase error. The phase angle is fixed at $\phi = 2\pi/10$ so that results can be compared with those of Vreugdenhil [11]. Central

© 1998 John Wiley & Sons, Ltd.

differencing has the highest phase error, while the proposed method has the lowest phase error at low c_z. At high c_z all methods have similar phase error.

In the previous analysis we fixed $\theta = 0.5$ and found relations for β which satisfy von Neumann stability. Alternatively, the second-order spatial error could have been eliminated by fixing $\beta = 0$ and varying θ. However, an analysis for $\beta = 0$ and variable θ concludes that $\theta = 1$ must be chosen for $|c_z| > 2$, and for higher Courant number β must also be increased. Thus, varying θ with $\beta = 0$ cannot provide unconditional stability. For this reason, in addition to the reasons previously explained, this method uses $\theta = 0.5$ and β is varied to provide stability.

2.3. Matrix invertibility

The von Neumann stability analysis has provided relations for choosing β as a function of Courant number for $\theta \geq 0.5$. However, the invertibility of the matrix resulting from various choices of β or θ must also be proven. We will consider not only unidirectional flow, but all possible vertical flow configurations, such as diverging flow, converging flow and flow into or out of only one flux face (as occurs in the top and bottom cells of the water column). The β method for solving Equation (2) for variable velocity can be written as

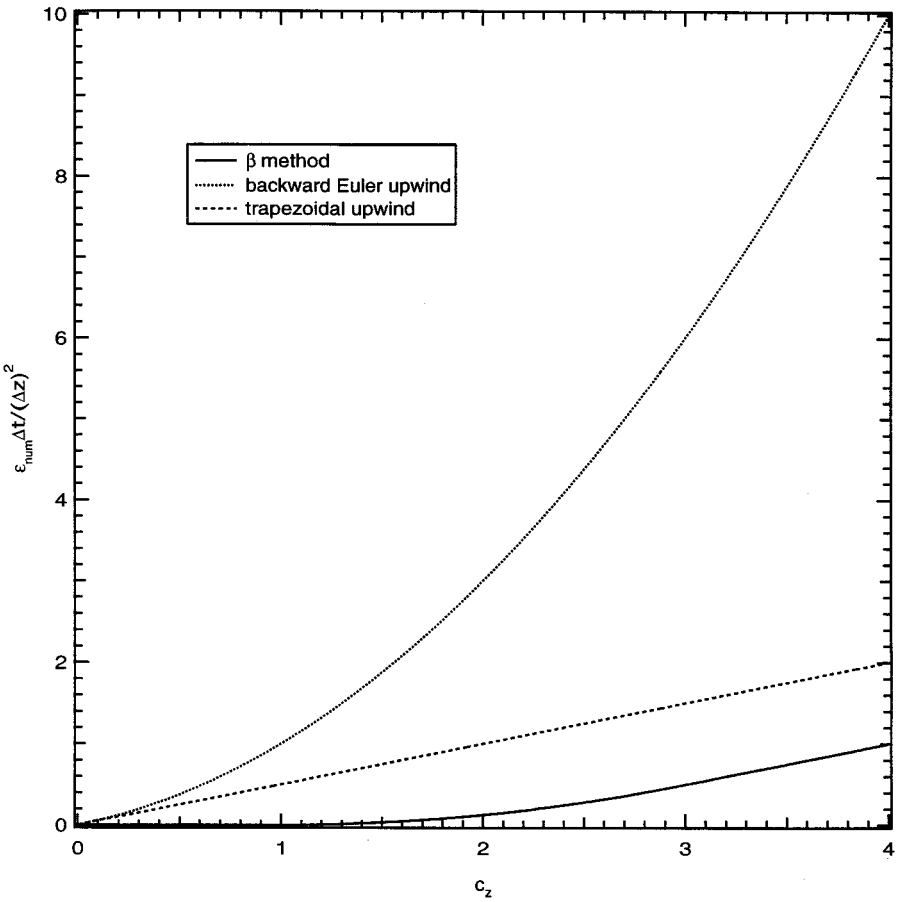

Figure 3. Variation of non-dimensionalized numerical diffusion coefficients with Courant number for different scalar advection schemes.

© 1998 John Wiley & Sons, Ltd.

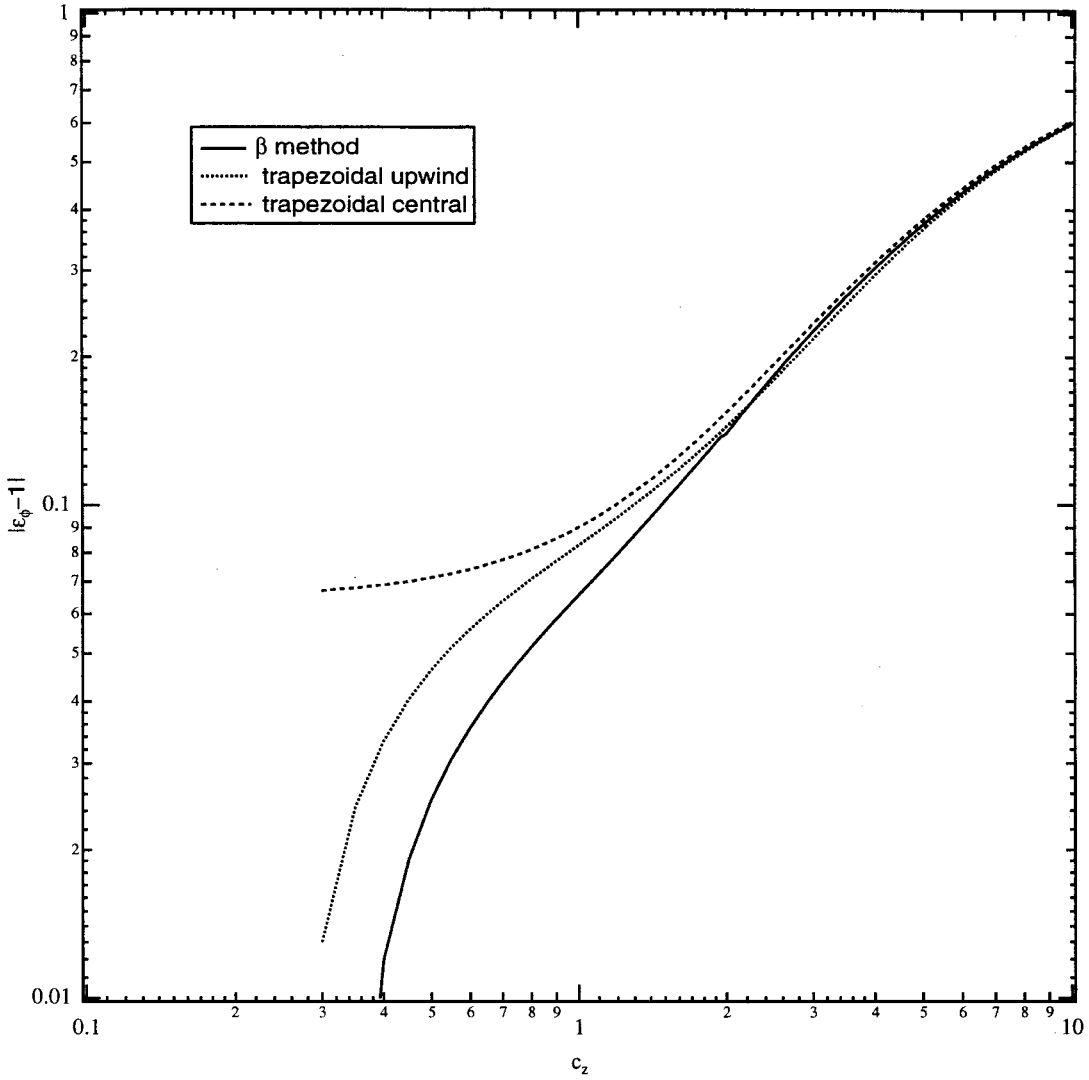

Figure 4. Variation of phase error with Courant number for a fixed phase angle, $\phi = 2\pi/10$, for different scalar advection schemes.

$$
\begin{aligned}
& s_k^{n+1} + \frac{\theta}{2}[\beta_{k+1/2}(c_{k+1/2} + |c_{k+1/2}|)s_k^{n+1} + \beta_{k+1/2}(c_{k+1/2} - |c_{k+1/2}|)s_{k+1}^{n+1} \\
& - \beta_{k-1/2}(c_{k-1/2} + |c_{k-1/2}|)s_{k-1}^{n+1} - \beta_{k-1/2}(c_{k-1/2} - |c_{k-1/2}|)s_k^{n+1} \\
& + (1 - \beta_{k+1/2})c_{k+1/2}(s_{k+1}^{n+1} + s_k^{n+1}) - (1 - \beta_{k-1/2})c_{k-1/2}(s_k^{n+1} + s_{k-1}^{n+1})] \\
& = s_k^n - \frac{(1-\theta)}{2}[\beta_{k+1/2}(c_{k+1/2} + |c_{k+1/2}|)s_k^n + \beta_{k+1/2}(c_{k+1/2} - |c_{k+1/2}|)s_{k+1}^n \\
& \quad - \beta_{k-1/2}(c_{k-1/2} + |c_{k-1/2}|)s_{k-1}^n - \beta_{k-1/2}(c_{k-1/2} - |c_{k-1/2}|)s_k^n \\
& \quad + (1 - \beta_{k+1/2})c_{k+1/2}(s_{k+1}^n + s_k^n) - (1 - \beta_{k-1/2})c_{k-1/2}(s_k^n + s_{k-1}^n)]
\end{aligned}
$$

© 1998 John Wiley & Sons, Ltd.

$$+\frac{1}{16}(1-\beta_{k+1/2})[(c_{k+1/2}+|c_{k+1/2}|)(s^n_{k-1}+s^n_{k+1}-2s^n_k)$$
$$+(c_{k+1/2}-|c_{k+1/2}|)(s^n_k+s^n_{k+2}-2s^n_{k+1})]$$
$$-\frac{1}{16}(1-\beta_{k-1/2})[(c_{k-1/2}+|c_{k-1/2}|)(s^n_{k-2}+s^n_k-2s^n_{k-1})$$
$$+(c_{k-1/2}-|c_{k-1/2}|)(s^n_{k-1}+s^n_{k+1}-2s^n_k)] \tag{22}$$

Note that when variable velocities are considered, β also varies in space and time. One equation for s^{n+1} is defined for each computational cell, thus resulting in a tridiagonal matrix. In order to simplify the notation, c_z is simply referred to as c in Equation (22) and throughout this section.

Diagonal dominance of the matrix guarantees invertibility. However, in the case of converging flow ($c_{k-1/2}>0$, $c_{k+1/2}<0$), the diagonal dominance condition for this matrix would require a β larger than that required for stability. Thus, we will analyze a Gaussian elimination algorithm for the solution of the tridiagonal system and show a sufficient condition for assuring a solution, which is generally met by the previous choice of $\theta=0.5$ in β in Equation (21).

For a generic tridiagonal system,

$$\mathbf{A}\bar{s}=\bar{b} \tag{23}$$

where

$$\mathbf{A}=\begin{pmatrix} a_{m,m} & a_{m,m+1} & 0 & & 0 \\ a_{m+1,m} & a_{m+1,m+1} & a_{m+1,m+2} & & 0 \\ \cdot & \cdot & \cdot & \cdot & \cdot \\ \cdot & \cdot & \cdot & \cdot & \cdot \\ \cdot & \cdot & \cdot & \cdot & \cdot \\ 0 & & & a_{M,M-1} & a_{M,M} \end{pmatrix} \tag{24}$$

and $\bar{s}$ and $\bar{b}$ are vectors with indices ranging from m to M, thus of length $(M-m+1)$. The elimination step of the Gaussian elimination algorithm can be written as follows,

$$d_m=a_{m,m}, \tag{25}$$

$$d_k=a_{k,k}-a_{k,k-1}\frac{a_{k-1,k}}{d_{k-1}}, \quad k=m+1,\ldots,M \tag{26}$$

where d_k is the diagonal of row k after the elimination step is complete. A triangular matrix with non-zero values on the main diagonal can always be inverted. Thus, it is sufficient to prove that, once the lower diagonal has been eliminated, the resulting upper triangular system has non-zero values on the diagonal. Therefore, sufficient conditions for invertibility are that $a_{m,m}>0$ and, that given $d_{k-1}>0$, we can prove that $d_k>0$. From Equation (22), the matrix coefficients of row k are

$$a_{k,k-1}=\frac{\theta}{2}[\beta_{k-1/2}(-c_{k-1/2}-|c_{k-1/2}|)-(1-\beta_{k-1/2})c_{k-1/2}], \tag{27}$$

© 1998 John Wiley & Sons, Ltd.

$$a_{k,k} = 1 + \frac{\theta}{2}[\beta_{k+1/2}(c_{k+1/2} + |c_{k+1/2}|) - \beta_{k-1/2}(c_{k-1/2} - |c_{k-1/2}|) + (1 - \beta_{k+1/2})c_{k+1/2} - (1 - \beta_{k-1/2})c_{k-1/2}], \tag{28}$$

$$a_{k,k+1} = \frac{\theta}{2}[\beta_{k+1/2}(c_{k+1/2} - |c_{k+1/2}|) + (1 - \beta_{k+1/2})c_{k+1/2}], \tag{29}$$

where $c_{k+1/2} = w_{k+1/2}\Delta t/\Delta z_k^{n+1}$. The resulting expression for the product $-a_{k,k-1}a_{k-1,k}$ is

$$\frac{1}{4}\theta^2 c_{k+1/2}^2(1 - \beta_{k-1/2}^2), \tag{30}$$

which is non-negative for all valid values of β and θ. In this case, Equation (30) is positive and a sufficient condition to ensure invertibility is that the original main diagonal is non-negative. The velocity configuration which results in the minimum main diagonal is converging flow ($w_{k-1/2} > 0$, $w_{k+1/2} < 0$). For converging flow, the condition for invertibility is

$$1 + \frac{\theta}{2}(1 - \beta_{k+1/2})c_{k+1/2} - \frac{\theta}{2}(1 - \beta_{k-1/2})c_{k-1/2} \geq 0. \tag{31}$$

If we define

$$c_{\max} = \max(|c_{k-1/2}|, |c_{k+1/2}|, |c_{k+3/2}|), \tag{32}$$

we obtain the following condition for invertibility

$$\beta_{k+1/2} \geq 1 - \frac{1}{\theta c_{\max}}, \tag{33}$$

This condition is sufficient, but not necessary, to guarantee invertibility. Note that decreasing θ improves the invertibility of the matrix, and thus allows smaller β values to be chosen.

In conclusion, for $\theta = 0.5$, sufficient conditions for invertibility and von Neumann stability are:

$$\beta(c_{\max}) = \begin{cases} 0 & |c_{\max}| \leq 1 \\ \dfrac{(|c_{\max}| - 1)^2}{4|c_{\max}|} & 1 \leq |c_{\max}| \leq 3 \\ \dfrac{|c_{\max}| - 2}{|c_{\max}|} & |c_{\max}| \geq 3 \end{cases} \tag{34}$$

2.4. Addition of diffusion terms

For this section, the scalar transport equation with non-zero diffusion

$$\frac{\partial s}{\partial t} + \frac{\partial (ws)}{\partial z} = \frac{\partial}{\partial z}\left(\epsilon_v \frac{\partial s}{\partial z}\right) \tag{35}$$

is discretized using the β method for the advection term and Crank–Nicolson for the diffusion term in the following way:

$$s_k^{n+1} = s_k^n - (c_{k+1/2}s_u - c_{k-1/2}s_l) + \frac{e_{k+1/2}}{2}(s_{k+1}^{n+1} - s_k^{n+1}) - \frac{e_{k-1/2}}{2}(s_k^{n+1} - s_{k-1}^{n+1}) + \frac{e_{k+1/2}}{2}(s_{k+1}^n - s_k^n) - \frac{e_{k-1/2}}{2}(s_k^n - s_{k-1}^n) \tag{36}$$

© 1998 John Wiley & Sons, Ltd.

where s_u and s_l are interpolated based on the β method as in Equation (22) and $e = \epsilon_v \Delta t/(\Delta z)^2$. The vertical diffusion term is treated implicitly to avoid a restrictive stability condition based on Δz.

The implementation of diffusion with the β method allows for lower values of β to satisfy von Neumann stability than those given by Equation (34). In addition, the resulting matrix is again tridiagonal and invertible for any e. In the presence of diffusion the matrix is diagonally dominant for

$$e_{k-1/2} > \theta(1 - \beta_{k-1/2})|c_{k-1/2}|. \tag{37}$$

An analysis of the Gaussian elimination algorithm analogous to that carried out for the zero diffusion case yields

$$-a_{k,k-1}a_{k-1,k} = \left(\frac{\theta}{2}c_{k-1/2}\right)^2 - \left(\frac{\theta}{2}\beta_{k-1/2}|c_{k-1/2}| + \frac{e_{k-1/2}}{2}\right)^2 \tag{38}$$

so that using this approach, a sufficient condition for invertibility is

$$\frac{e_{k-1/2}}{2} \leq \frac{\theta}{2}(1 - \beta_{k-1/2})|c_{k-1/2}|. \tag{39}$$

Therefore, there is invertibility for all values of the diffusion coefficient, given that β is specified by Equation (34). Thus, the vertical diffusion term does not add computational difficulty. For this reason and for the sake of a simpler presentation, scalar diffusion will not be considered further.

3. ONE-DIMENSIONAL TEST CASES

Before incorporating the β method into a three-dimensional model, the results of some simple one-dimensional test cases will be presented. The β method will be compared with two common implicit methods, upwind differencing and central differencing. The trapezoidal method is used for time advancement in all cases.

In the first case, the grid spacing is varied in order to examine the grid convergence of this method for the transport of a Gaussian concentration profile with a standard deviation of 2 m over a distance of 50 m. In all simulations, $w = 1$ m s^{-1} and $\Delta t = 0.1$ s. Figure 5 illustrates that for $\Delta z > 0.1$ m ($c_z < 1$), this method converges roughly as $(\Delta z)^2$. However, when $\Delta z < 0.1$ m ($c_z > 1$), some upwind differencing is added to the transport computations and the error actually increases with grid refinement due to increased numerical diffusion. The variation of RMS error with grid spacing for upwind differencing is also provided for reference. For $c_z < 1$ the error for the β method is one order of magnitude lower than the error for upwind differencing. In the range of very high Courant numbers ($c_z > 10$) the error of the β method asymptotically approaches the error of upwind differencing, which decreases as Δz. In the region of moderately high Courant numbers ($1 < c_z < 10$), the β method is always much more accurate than upwind differencing. The error associated with central differencing is higher than the error associated with the β method for $c_z < 2$. For higher Courant number, central differencing yields lower error. However, invertibility is not guaranteed for central differencing if $c_z > 2$.

The second test case was used by Leonard [12] to compare many explicit conservative advection schemes. In this case, three test profiles travel a distance of 45 Δz at $c_z = 0.5$ with $w = 1$ m s^{-1}, $\Delta z = 0.01$ m and $\Delta t = 0.005$ s. While this low Courant number test case is not

© 1998 John Wiley & Sons, Ltd.

appropriate for an unconditionally stable method, such as the β method, it is provided to compare the performance of this method with conditionally stable explicit methods at a low Courant number. One explicit method, QUICKEST [4], is included in the comparison. The explicit QUICK [4] method is more closely related to the proposed method but is not stable for pure convection, and therefore is not included.

The concentration units which will be used in all test cases is 'parts per thousand' (ppt), which are often used to report salinity values. One part per thousand represents 1 g solute per 1000 g solution. The first test profile is a unit step, in which values to the left of the step, including the boundary value, are 1.0 ppt and values to the right of the step are 0.0 ppt. The second test profile, a sine-squared wave of width 20 Δz, follows after a separation of 40 Δz. This profile is described by the formula

$$s = \sin^2\left(\frac{\pi z}{20\Delta z}\right) \quad \text{for } 0 \le z \le 20\Delta z. \tag{40}$$

The third test profile, a semi-ellipse of width 20 Δz, centered at z_c, follows after a separation of 30 Δz. This profile is described by

$$s = \sqrt{1 - (z - z_c)^2/(10\Delta z)^2} \quad \text{for } 0 \le z \le 20\Delta z. \tag{41}$$

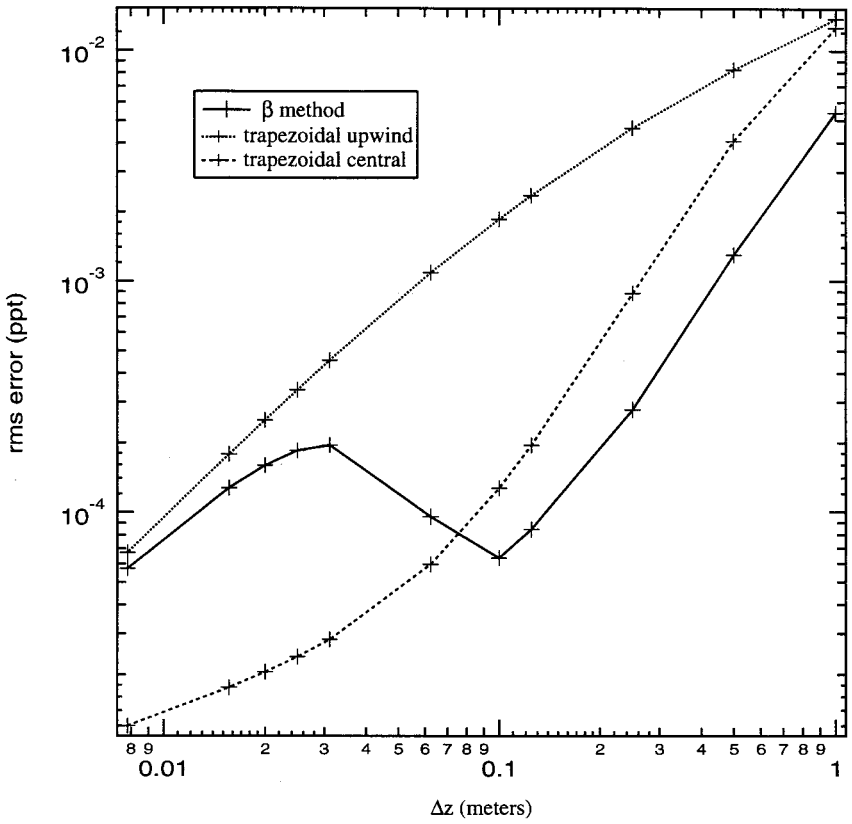

Figure 5. Variation of RMS error in scalar concentration with grid spacing.

© 1998 John Wiley & Sons, Ltd.

Table I. Comparison of advection schemes for uniform grid test case

Profile	Step		Sine-squared		Semi-ellipse		Total CPU
Scheme	$\mathscr{E}$	$\mathscr{W}$	$\mathscr{E}$	$\mathscr{W}$	$\mathscr{E}$	$\mathscr{W}$	
Upwind trapezoidal	5.34	1.88	6.74	1.90	7.98	2.02	0.047
Central trapezoidal	6.99	6.75	2.95	2.43	3.77	2.65	0.073
β method	2.21	2.22	0.78	0.40	1.90	1.77	0.127
QUICKEST	1.41	1.74	0.26	0.15	1.16	1.29	0.022

The results of this test case are shown in Figure 6. Clearly the two methods which perform best are QUICKEST and the β method. As expected, the solution given by first-order upwind differencing is highly diffused and the central differencing solution has strong oscillations. For ease of comparison, the quantitative measures of error used are also taken from Leonard [12]. Total absolute error is defined as

$$\mathscr{E} = \sum_{k=1}^{N} |\varepsilon_k|, \tag{42}$$

where ε is the local error at each node

$$\varepsilon = s_{\text{computed}} - s_{\text{exact}}. \tag{43}$$

The other measure, which Leonard [12] calls WAVINESS is

$$\mathscr{W} = \sum_{k=1}^{N} |\varepsilon_{k+1} - \varepsilon_k|. \tag{44}$$

As shown in Table I, the most accurate scheme by both error measures is QUICKEST, which also requires the least computational time. QUICKEST, however, is unstable for $|c_z| > 1$. In contrast, the implicit methods used are unconditionally stable. Because computing vertical scalar advection requires only a small fraction of the total computational cost in a three-dimensional hydrodynamic model, the increased time step allowed by the implicit methods will result in large computational savings.

The third test case is appropriate for the β method because a range of c_z is present, exceeding 1.0 in some regions, while low Courant numbers are more common within the domain, as occurs when this method is applied to study tidal hydrodynamics. The grid was divided into three sections; a uniform coarse grid section with a grid spacing of 0.1 m, a stretched grid with a minimum grid spacing of 0.01 m and another uniform coarse grid section with a grid spacing of 0.1 m. A constant velocity of 1.0 m s^{-1} was used. The variation of grid spacing with z is shown in Figure 7. For the comparison between upwind and central differencing $\Delta t = 0.04$ s was used, providing a maximum Courant number (c_{MAX}) of 4. The same profiles were used in this test case as in the previous test case. Transport results are shown after these profiles have traveled a distance of 40 m, through 564 grid cells, an order of magnitude more grid cells than in the previous test case.

We can see from Figure 8 that the β method is much more accurate than both upwind differencing and central differencing for the simulation with $c_{\text{MAX}} = 4$. This method retains the peaks of these profiles quite well, as does central differencing, but yields lower phase error and smaller oscillations than central differencing. In addition, the oscillations caused by the β method do not persist after the profiles have passed, while central differencing leaves oscillations throughout the entire advection region.

© 1998 John Wiley & Sons, Ltd.

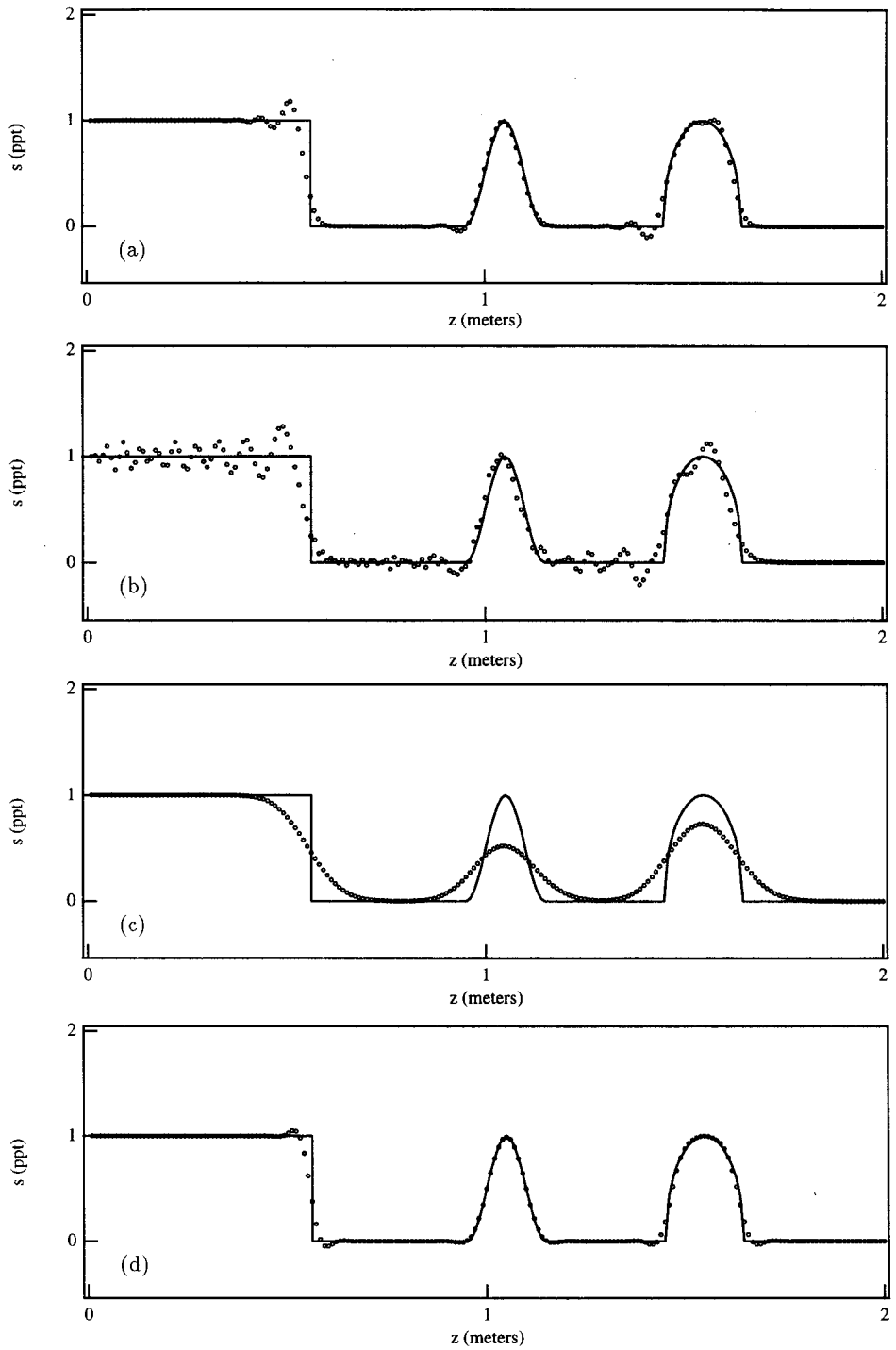

Figure 6. Scalar concentration after advection of test profiles through a uniform grid: (a) the β method, (b) trapezoidal central, (c) trapezoidal upwind, (d) QUICKEST.

© 1998 John Wiley & Sons, Ltd.

Table II shows the total errors using the same error measures as in the first test case, however, for this test case, only the total error for the three test profiles together is presented. Results are given for $c_{MAX} = 1$, $c_{MAX} = 4$ and $c_{MAX} = 8$. Errors for each profile are not presented individually because there are no longer clear boundaries between adjacent profiles for upwind and central differencing. The β method is clearly the most accurate of these simple implicit methods and its accuracy does not degrade rapidly for $c_{MAX} > 1$. Therefore, this method will be implemented in order to compute vertical scalar advection in a three-dimensional model.

4. OUTLINE OF THE HYDRODYNAMIC MODEL TRIM-3D

The β method will now be applied to compute vertical scalar advection in a three-dimensional hydrodynamic model. In this section the governing equations of the three-dimensional model TRIM-3D [1] will be presented and the numerical approach used to solve these equations will be outlined.

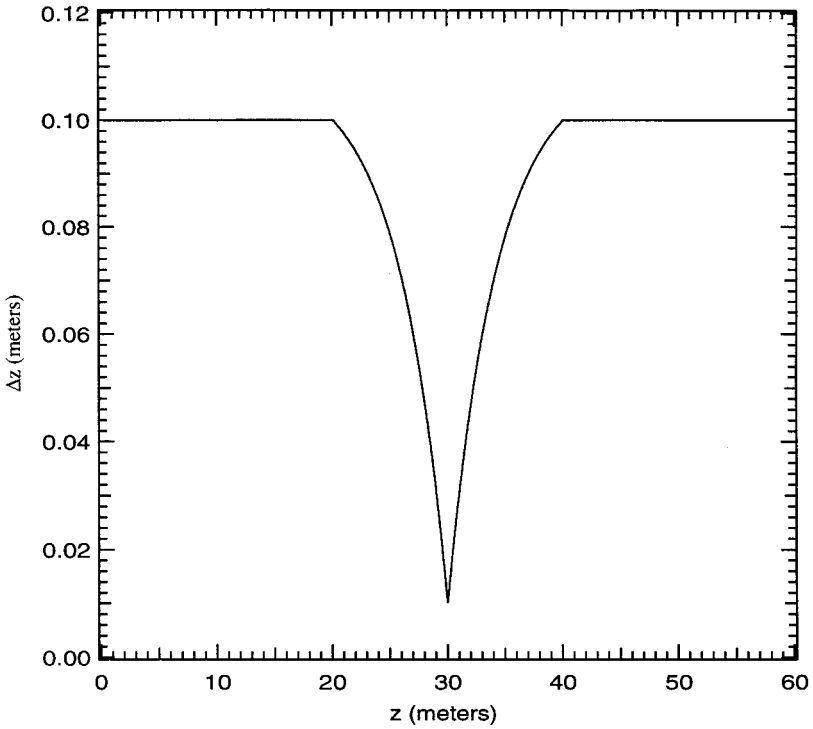

Figure 7. Variation of grid spacing in stretched grid: the grid consists of two uniform grid regions with $\Delta z = 0.1$ m and a stretched grid section with a minimum Δz of 0.01 m.

© 1998 John Wiley & Sons, Ltd.

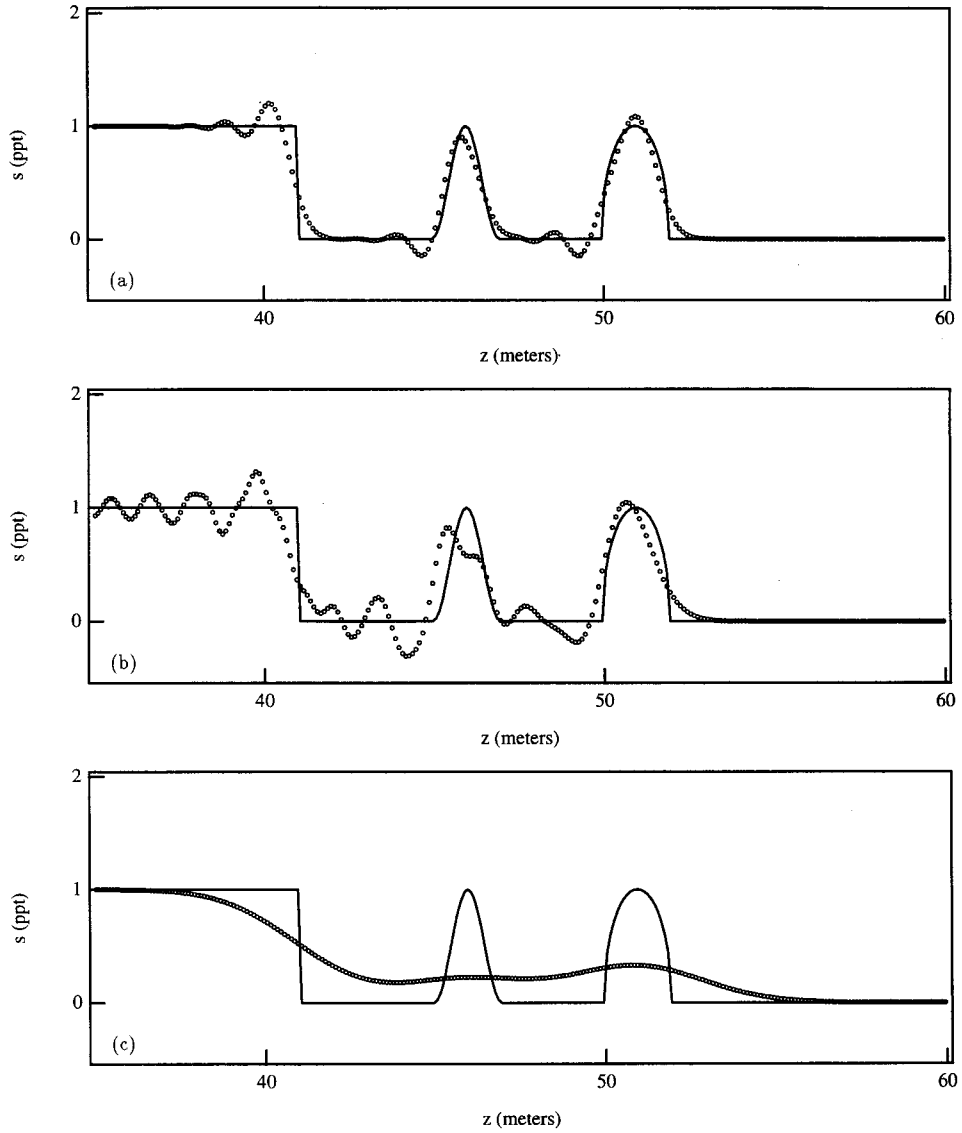

Figure 8. Scalar concentration after advection of test profiles through a stretched grid: (a) the β method, (b) trapezoidal central, (c) trapezoidal upwind.

4.1. Governing equations

The governing equations of TRIM-3D are the Reynolds averaged shallow water equations

$$\frac{\partial u}{\partial t}+u\frac{\partial u}{\partial x}+v\frac{\partial u}{\partial y}+w\frac{\partial u}{\partial z}=-g\frac{\partial \eta}{\partial x}-\frac{g}{\rho_o}\frac{\partial}{\partial x}\left(\int_z^{\eta}\rho'\,\mathrm{d}z\right)+v_{\mathrm{h}}\left(\frac{\partial^2 u}{\partial x^2}+\frac{\partial^2 u}{\partial y^2}\right)+\frac{\partial}{\partial z}\left(v_{\mathrm{v}}\frac{\partial u}{\partial z}\right)+fv, \tag{45}$$

© 1998 John Wiley & Sons, Ltd.

$$\frac{\partial v}{\partial t}+u\frac{\partial v}{\partial x}+v\frac{\partial v}{\partial y}+w\frac{\partial v}{\partial z}=-g\frac{\partial \eta}{\partial y}-\frac{g}{\rho_o}\frac{\partial}{\partial y}\left(\int_z^{\eta}\rho'\,\mathrm{d}z\right)+\nu_{\mathrm{h}}\left(\frac{\partial^2 v}{\partial x^2}+\frac{\partial^2 v}{\partial y^2}\right)+\frac{\partial}{\partial z}\left(\nu_{\mathrm{v}}\frac{\partial v}{\partial z}\right)-fu, \tag{46}$$

$$\frac{\partial u}{\partial x}+\frac{\partial v}{\partial y}+\frac{\partial w}{\partial z}=0, \tag{47}$$

where $u(x, y, z, t)$, $v(x, y, z, t)$, $w(x, y, z, t)$ are the velocity components in the horizontal x-, y-directions and vertical z-direction, respectively, $\eta(x, y, t)$ is the water surface elevation above an undisturbed water level, f is the Coriolis parameter, ν_{h} is the constant horizontal eddy viscosity, $\nu_{\mathrm{v}}(x, y, z, t)$ is the vertical eddy viscosity, ρ_o is a constant reference density, $\rho'(x, y, z, t)$ is the local variation from the reference density, t is time and g is gravitational acceleration.

Equation (47) can be integrated over the water column and combined with the kinematic boundary condition at the free surface to obtain

$$\frac{\partial \eta}{\partial t}+\frac{\partial}{\partial x}\left[\int_{-H^{\circ}}^{\eta}u\,\mathrm{d}z\right]+\frac{\partial}{\partial y}\left[\int_{-H^{\circ}}^{\eta}v\,\mathrm{d}z\right]=0, \tag{48}$$

where $H^{\circ}(x, y)$ is the depth of the bottom boundary measured from the undisturbed free surface.

The conservative scalar transport Equation (1) without turbulent diffusion terms is

$$\frac{\partial s}{\partial t}+\frac{\partial (us)}{\partial x}+\frac{\partial (vs)}{\partial y}+\frac{\partial (ws)}{\partial z}=0. \tag{49}$$

For non-passive scalars an equation of state, $\rho=\rho(s)$, is used to relate density to scalar concentration. With appropriate initial and boundary conditions, the set of equations (45)–(49) form an initial-boundary value problem for three-dimensional shallow water flow, which is solved with the TRIM-3D method.

4.2. Numerical method

TRIM-3D is a semi-implicit finite difference scheme which solves the three-dimensional shallow water equations on a staggered grid. A Θ factor which varies between 1/2 and 1 is introduced to control the degree of implicitness of the velocities in the free surface equation and the barotropic terms in the momentum equations. It has been shown by Casulli and Cattani [1] that the highest accuracy and efficiency of the method is achieved for $\Theta=1/2$. The advective terms in the momentum equations are handled using the Eulerian–Lagrangian Method [2].

The finite difference form of the hydrodynamic equations can be written

Table II. Comparison of advection schemes for stretched grid test case

Courant number	$c_{\mathrm{MAX}}=1$		$c_{\mathrm{MAX}}=4$		$c_{\mathrm{MAX}}=8$	
Scheme	$\mathscr{E}$	$\mathscr{W}$	$\mathscr{E}$	$\mathscr{W}$	$\mathscr{E}$	$\mathscr{W}$
Upwind trapezoidal	0.0556	0.00727	0.0556	0.00727	0.0554	0.00727
Central trapezoidal	0.0432	0.02310	0.0433	0.02305	0.0442	0.02178
β method	0.0113	0.00645	0.0140	0.00744	0.0205	0.00918

© 1998 John Wiley & Sons, Ltd.

$$u^{n+1}_{i+1/2,j,k} = Fu^{n}_{i+1/2,j,k} - g\frac{\Delta t}{\Delta x}\left(\eta^{n+\Theta}_{i+1,j} - \eta^{n+\Theta}_{i,j}\right) + \Delta t\,\frac{v_{i,j,k+1/2}\dfrac{u^{n+1}_{i+1/2,j,k+1} - u^{n+1}_{i+1/2,j,k}}{\Delta z^{n}_{i+1/2,j,k+1/2}} - v_{i,j,k-1/2}\dfrac{u^{n+1}_{i+1/2,j,k} - u^{n+1}_{i+1/2,j,k-1}}{\Delta z^{n}_{i+1/2,j,k-1/2}}}{\Delta z^{n}_{i+1/2,j,k}}, \tag{50}$$

$$v^{n+1}_{i,j+1/2,k} = Fv^{n}_{i,j+1/2,k} - g\frac{\Delta t}{\Delta y}\left(\eta^{n+\Theta}_{i,j+1} - \eta^{n+\Theta}_{i,j}\right) + \Delta t\,\frac{v_{i,j,k+1/2}\dfrac{v^{n+1}_{i,j+1/2,k+1} - v^{n+1}_{i,j+1/2,k}}{\Delta z^{n}_{i,j+1/2,k+1/2}} - v_{i,j,k-1/2}\dfrac{v^{n+1}_{i,j+1/2,k} - v^{n+1}_{i,j+1/2,k-1}}{\Delta z^{n}_{i,j+1/2,k-1/2}}}{\Delta z^{n}_{i,j+1/2,k}}, \tag{51}$$

$$\eta^{n+1}_{i,j} = \eta^{n}_{i,j} - \frac{\Delta t}{\Delta x}\left[\sum_{k=m}^{M}\Delta z^{n}_{i+1/2,j,k}u^{n+\Theta}_{i+1/2,j,k} - \sum_{k=m}^{M}\Delta z^{n}_{i-1/2,j,k}u^{n+\Theta}_{i-1/2,j,k}\right] - \frac{\Delta t}{\Delta y}\left[\sum_{k=m}^{M}\Delta z^{n}_{i,j+1/2,k}v^{n+\Theta}_{i,j+1/2,k} - \sum_{k=m}^{M}\Delta z^{n}_{i,j-1/2,k}v^{n+\Theta}_{i,j-1/2,k}\right], \tag{52}$$

where m and M denote the bottom and top computational cells in a water column, respectively, Fu and Fv represent the explicit terms, and $\Delta z_{i\pm1/2,j,k}$ and $\Delta z_{i,j\pm1/2,k}$ are the heights of the flux faces, which are equal to $\Delta z_{i,j,k}$, except at the bottom and top cells, and $u^{n+\Theta}$ denotes

$$u^{n+\Theta} = \Theta u^{n+1} + (1-\Theta)u^{n}.$$

The new free surface elevation is computed by substituting Equations (50) and (51) into (52), resulting in a pentadiagonal matrix which is symmetric and positive definite, and thus can be solved efficiently using a conjugate gradient method [1]. After the new water surface elevation is computed, the horizontal velocities are calculated using Equations (50) and (51). Next, the vertical velocity w is updated using the continuity equation as follows:

$$w^{n+\Theta}_{i,j,k+1/2} = w^{n+\Theta}_{i,j,k-1/2} - \frac{\Delta z^{n}_{i+1/2,j,k}u^{n+\Theta}_{i+1/2,j,k} - \Delta z^{n}_{i-1/2,j,k}u^{n+\Theta}_{i-1/2,j,k}}{\Delta x} - \frac{\Delta z^{n}_{i,j+1/2,k}v^{n+\Theta}_{i,j+1/2,k} - \Delta z^{n}_{i,j-1/2,k}v^{n+\Theta}_{i,j-1/2,k}}{\Delta y}. \tag{53}$$

The numerical algorithm conserves water mass, allows wetting and drying of tidal flats and reduces to the two-dimensional TRIM-2D method [13] if one vertical layer is specified.

4.3. Conservative scalar transport coupled to TRIM-3D

The advective transport Equation (49) is not in a form directly useful for free surface applications. In simulations with TRIM-3D, the vertical grid spacing, Δz, changes in time as the free surface moves. This is reflected by the layer averaged advective transport equation for layer k,

$$\frac{\partial(s\Delta z)}{\partial t} + \frac{\partial(us\Delta z)}{\partial x} + \frac{\partial(vs\Delta z)}{\partial y} + (ws)_{k+1/2} - (ws)_{k-1/2} = 0, \tag{54}$$

while at the top cell, after layer averaging and application of the kinematic boundary condition at the free surface, Equation (49) becomes

© 1998 John Wiley & Sons, Ltd.

$$\frac{\partial(s\Delta z)}{\partial t}+\frac{\partial(us\Delta z)}{\partial x}+\frac{\partial(vs\Delta z)}{\partial y}-(ws)_{k-1/2}=0, \tag{55}$$

indicating that there is no scalar flux through the free surface.

Consistency with the continuity equation requires that the amount of water entering through each flux face, as determined by Equation (52), is equal to the amount that enters each flux face in the transport equation. Thus, the time level and location of u, v, w and Δz in the transport equation are chosen to be the same as in Equation (52), and the concentration of the scalar at the flux face is interpolated from the values defined at the center of the staggered grid according to an advective scheme. The only difference between the various one-step conservative advection schemes which are consistent with the continuity equation, is the method used to interpolate the concentrations to the flux faces. A general finite difference form of Equation (54) is

$$\begin{aligned} s^{n+1}_{i,j,k}\Delta z^{n+1}_{i,j,k} = {} & s^{n}_{i,j,k}\Delta z^{n}_{i,j,k}-\frac{\Delta t}{\Delta x}(\Delta z^{n}_{i+1/2,j,k}u^{n+\Theta}_{i+1/2,j,k}s_{\mathrm{e}}-\Delta z^{n}_{i-1/2,j,k}u^{n+\Theta}_{i-1/2,j,k}s_{\mathrm{w}}) \\ & -\frac{\Delta t}{\Delta y}(\Delta z^{n}_{i,j+1/2,k}v^{n+\Theta}_{i,j+1/2,k}s_{\mathrm{n}}-\Delta z^{n}_{i,j-1/2,k}v^{n+\Theta}_{i,j-1/2,k}s_{\mathrm{s}}) \\ & -\Delta t(w^{n+\Theta}_{i,j,k+1/2}s_{\mathrm{u}}-w^{n+\Theta}_{i,j,k-1/2}s_{\mathrm{l}}), \end{aligned} \tag{56}$$

where s_{e}, s_{w}, s_{n}, s_{s}, s_{u} and s_{l} are the concentration values interpolated onto the flux faces respectively labeled east, west, north, south, upper and lower. The method of interpolation and time levels associated with s_{e}, s_{w}, s_{n}, s_{s}, s_{u} and s_{l} are intentionally not specified. The proposed method is conservative, which is guaranteed in this equation provided $(s_{\mathrm{w}})_{i+1/2,j,k}=(s_{\mathrm{e}})_{i-1/2,j,k}$, $(s_{\mathrm{s}})_{i,j+1/2,k}=(s_{\mathrm{n}})_{i,j-1/2,k}$ and $(s_{\mathrm{l}})_{i,j,k+1/2}=(s_{\mathrm{u}})_{i,j,k-1/2}$. In a uniform scalar field of concentration s, the value interpolated to all flux faces will be s. Thus, for uniform concentration $s=1$, the result of summing Equation (56) over the water column and substituting Equation (52) is $s^{n+1}=1$. Without this guarantee of consistency, an initially uniform concentration field in a closed basin will generally become non-uniform.

The β method was used to interpolate the concentration to the 'upper' flux face, s_{u}, such that for positive velocity

$$\begin{aligned} (s_{\mathrm{u}})_{i,j,k+1/2} = {} & \frac{1}{2}\beta_{i,j,k+1/2}(s^{n+1}_{i,j,k}+s^{n}_{i,j,k}) \\ & +(1-\beta_{i,j,k+1/2})\left(\frac{1}{4}s^{n+1}_{i,j,k+1}+\frac{1}{4}s^{n+1}_{i,j,k}+\frac{1}{8}s^{n}_{i,j,k+1}+\frac{1}{2}s^{n}_{i,j,k}-\frac{1}{8}s^{n}_{i,j,k-1}\right), \end{aligned} \tag{57}$$

s_{u} is defined from $k=m+1/2$ to $k=M-1/2$, where m and M are the k indices of the bottom and top cells respectively. This is the appropriate range of values for k, because there is no scalar flux through the free surface or the bottom boundary. β is chosen at each flux face, $m+1/2\le k\le M-1/2$, based on the local vertical Courant number, c_z, to satisfy Equation (34). The flux faces of the top ($k=M-1/2$) and bottom ($k=m+1/2$) cells of the water column are treated slightly differently. At $k=m+1/2$ the interpolation formula (57), used to evaluate $(s_{\mathrm{u}})_{i,j,m+1/2}$, will include $s_{i,j,m-1}$. However, $s_{i,j,m-1}$ is not a valid cell. For this reason, the 'correction' term

$$\frac{1}{8}(1-\beta)(s^{n}_{i,j,k-1}-2s^{n}_{i,j,k}+s^{n}_{i,j,k+1}), \tag{58}$$

© 1998 John Wiley & Sons, Ltd.

is not included in the interpolation formula in the bottom cell for positive velocities. Similarly, this term is not included at the top cell for negative velocities. The resulting interpolation formula at these flux faces is a combination of central differencing and upwind differencing. For each water column, a system of $(M-m+1)$ equations leads to a set of N_xN_y tridiagonal matrices, where N_x is the number of grid cells in the x-direction and N_y is the number of grid cells in the y-direction. Invertibility is guaranteed for each matrix and the overall method is stable under stability conditions which will be outlined next. Furthermore, wetting and drying of computational cells is allowed for hydrodynamics and scalar transport [14].

5. STABILITY CONDITIONS FOR THE THREE-DIMENSIONAL MODEL

The stability of the TRIM-3D model is independent of the free surface wave speed. However, the explicit treatment of the horizontal viscosity terms results in the stability condition [1]

$$\Delta t \leq \left[2\nu_h \left(\frac{1}{\Delta x^2} + \frac{1}{\Delta y^2} \right) \right]^{-1}. \tag{59}$$

When transport of a non-passive scalar (e.g. salt) is modeled, the momentum equations and the scalar transport equations are coupled through an equation of state. A CFL condition must then be imposed, independent of the transport scheme used, based on the speed of internal wave propagation. The speed of propagation of internal waves for a two-layer system is

$$u_{\text{int}} = \sqrt{g' \frac{h_1 h_2}{H}} \tag{60}$$

where h_1 is the thickness of upper layer, h_2 is the thickness of the lower layer, $H = h_1 + h_2$ is the total depth and

$$g' = g \frac{(\rho_2 - \rho_1)}{\rho_2}, \tag{61}$$

where ρ_1 is the density of the upper layer and ρ_2 is the density of the lower layer [15]. For a stable stratification, the maximum rate of internal wave propagation possible in the TRIM-3D model is

$$u_{\text{int}} = \sqrt{g \frac{(\rho_m - \rho_M)}{\rho_M} \frac{H}{4}}, \tag{62}$$

where ρ_m is the density in the bottom cell and ρ_M is the density in the top cell of the water column. The resulting CFL condition is

$$\Delta t \leq \frac{\Delta x \Delta y}{\sqrt{g \dfrac{(\rho_m - \rho_M)}{\rho_M} \dfrac{H}{4} (\Delta x^2 + \Delta y^2)}}. \tag{63}$$

Furthermore, since we are using explicit schemes for horizontal transport, a stability restriction based on the horizontal velocities will result. For example a sufficient condition for the stability of explicit first-order upwind differencing is $(|c_x| + |c_y|) < 1$ [16]. To avoid this time step limitation the horizontal advective terms may also be treated implicitly. However, in a strongly stratified flow Equation (63) can be as limiting as the stability limitation for the horizontal advective terms. Thus, there is not always a computational advantage to treating

© 1998 John Wiley & Sons, Ltd.

the horizontal terms implicitly. For this application we have chosen to treat horizontal advective terms explicitly. If time splitting of the horizontal and vertical transport steps was employed, the relation (34) could be used as it is and a stability restriction would result only from the explicit horizontal transport step.

In contrast, when scalar concentration is updated in a single step with explicit horizontal advection and the β method for vertical advection, the choice of β for stability is a function of the vertical and horizontal Courant numbers. The following is an example analysis with explicit upwind used for horizontal advection. The β method has also been applied successfully for vertical advection with other advection schemes applied in the horizontal. Since horizontal transport is not the focus of this paper, only the results with explicit upwind in the horizontal are presented.

The amplification factor of the β method with first-order upwind differencing in the horizontal is

$$G = \left[1 + \frac{c_z}{2}(\beta(1-\cos\alpha_z) + I\sin\alpha_z)\right]^{-1}$$
$$\left[1 - \frac{c_z}{2}(\beta(1-\cos\alpha_z) + I\sin\alpha_z) - \frac{1}{4}(1-\beta)c_z((1-\cos\alpha_z)^2 + I\sin\alpha_z(1-\cos\alpha_z))\right.$$
$$\left. + c_x(1-\cos\alpha_x + I\sin\alpha_x) + c_y(1-\cos\alpha_y + I\sin\alpha_y)\right], \tag{64}$$

where α_x, α_y and α_z are the phase angles in the x-, y-, and z-directions, respectively, and c_x, c_y and c_z are the Courant numbers in the x-, y- and z-directions. Furthermore we define

$$\tilde{G} = \left[1 + \frac{c_z}{2}(\beta(1-\cos\alpha_z) + I\sin\alpha_z)\right]^{-1}$$
$$\left[1 - \frac{c_z}{2}(\beta(1-\cos\alpha_z) + I\sin\alpha_z)\right.$$
$$- \frac{1}{4}(1-\beta)c_z((1-\cos\alpha_z)^2 + I\sin\alpha_z(1-\cos\alpha_z))$$
$$\left. + (c_x + c_y)(1-\cos\alpha_x + I\sin\alpha_x)\right]. \tag{65}$$

and assume that for all values of c_x, c_y, c_z and β

$$\sup_{\alpha_x,\alpha_y,\alpha_z} |G| \le \sup_{\alpha_x,\alpha_z} |\tilde{G}|. \tag{66}$$

This assumption has been checked for a wide range of c_x, c_y, c_z and β but has not been proven in general.

An analytical function, $\beta = \beta(|c_x| + |c_y|, |c_z|)$, which provides $|\tilde{G}| \le 1$ for all α_x and α_z has not been determined. Instead, Equation (65) was analyzed using a simple computer algorithm which finds the smallest value of β yielding $|\tilde{G}| \le 1$ for all possible phase angles given values of $|c_x| + |c_y|$ and $|c_z|$. Figure 9 shows various curves of $\beta = \beta(c_z)$ for a given $|c_x| + |c_y|$. β is specified in the following test cases using this information. Note that the one-dimensional β relation Equation (34) approaches $\beta = 1$ asymptotically. Thus, for all c_z, β could be chosen such that $|G| \le 1$. However, in multiple dimensions, for a given $|c_x| + |c_y|$, there is a limited range of c_z which provides $|G| \le 1$. For instance, for $|c_x| + |c_y| = 0.5$, the maximum c_z for which $|G| \le 1$ is $c_z = 4$. Thus, another time step limitation is imposed by this method when employed without time splitting.

© 1998 John Wiley & Sons, Ltd.

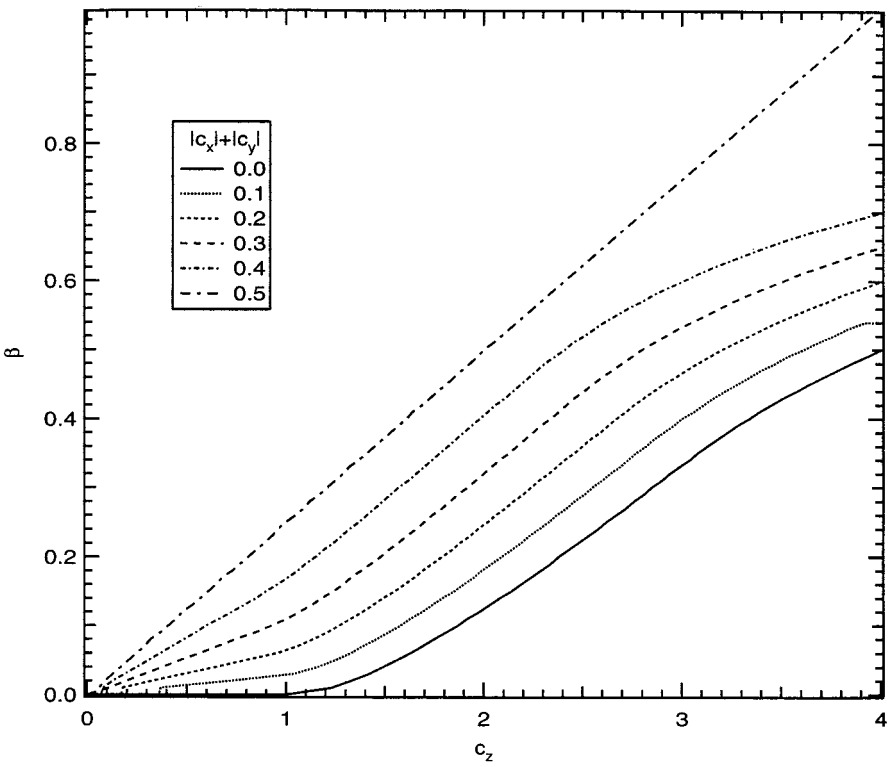

Figure 9. The minimum $\beta = f(|c_x| + |c_y|, c_z)$ which allows stability in the von Neumann sense.

6. TWO-DIMENSIONAL TEST CASE

The two-dimensional test case chosen is a seiche in a closed basin. TRIM-3D is applied with only one cell width in one horizontal direction, thus yielding a two-dimensional model with one horizontal co-ordinate (x) and one vertical co-ordinate (z). The initial condition, shown in Figure 10, employs a sin function of amplitude 1 m to specify the initial free surface. The horizontal grid spacing is 50 m with 40 grid cells in the horizontal, so that the period of the seiche is 400 s, with gravitational acceleration taken as 10 m s^{-2}. This steep free surface slope is used to provide high vertical velocities, as would be generated by bathymetric features in an estuary. The time step used in the simulation is 20 s and the uniform vertical grid spacing is 0.2 m, extending from the height of the free surface to a depth of 10 m from the undisturbed free surface. This vertical grid spacing provided a maximum vertical velocity of 0.0224 m s^{-1} corresponding to a Courant number of 2.24. Initially, there is a discontinuity in passive scalar concentration from 10 ppt to 20 ppt at a depth of 5 m and no diffusion term is present.

Figure 11 shows the scalar profile in a water column for the β method, trapezoidal upwind and trapezoidal central differencing, after 4.5 seiche periods. As expected, the results of upwind differencing are quite diffused and the results of central differencing contain strong oscillations. In contrast, the β method yields sharp gradients with relatively small oscillations throughout the seiche period. In all simulations scalar mass and water mass were conserved and computational time was nearly identical because the vertical scalar transport computations comprised a small fraction of the overall computational cost.

© 1998 John Wiley & Sons, Ltd.

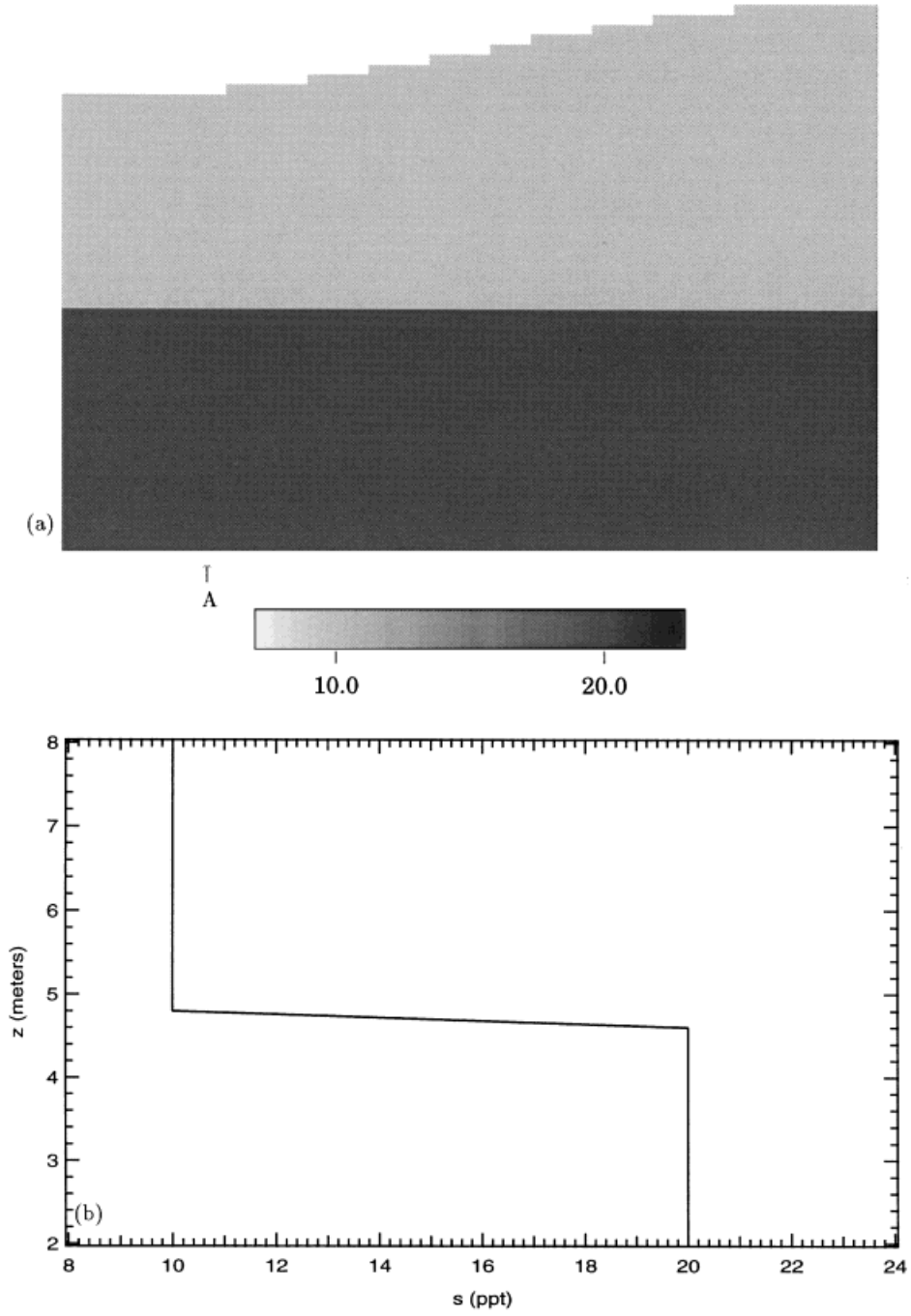

Figure 10. Initial scalar concentration for the two-dimensional test case of a seiche in a closed basin: (a) two-dimensional scalar field, (b) scalar profile of water column A.

© 1998 John Wiley & Sons, Ltd.

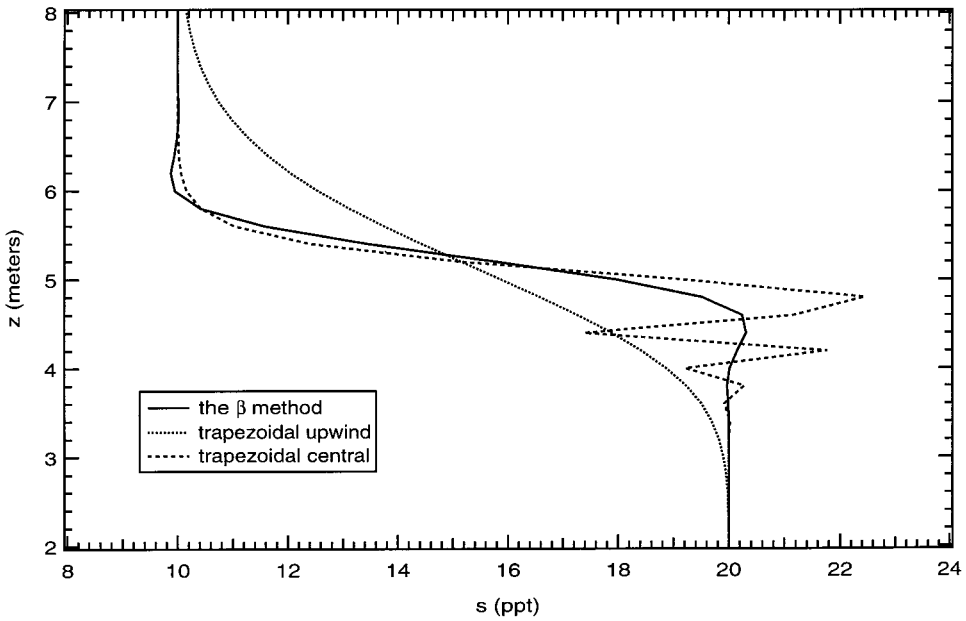

Figure 11. Scalar profile of water column A after 4.5 seiche periods.

7. THREE-DIMENSIONAL APPLICATION

The β method was applied to a three-dimensional transport simulation in South San Francisco Bay (SSFB). SSFB is a shallow, tidally dominated estuary with low direct freshwater input during most of the year. The hydrodynamic properties of SSFB are discussed by Conomos *et al.* [17], Cheng *et al.* [18], and other references contained therein. Due to discharge of contaminants in this region and the relatively long residence time of water, there is strong interest in the south end of SSFB.

The test case chosen for this study is transport simulation and is of practical importance because the wastewater treatment plants in the south end of SSFB discharge freshwater at the surface of the saline water of SSFB. The bathymetry of SSFB and the location of the discharge point are illustrated in Figure 12.

Tidal boundary conditions are applied at the northern end of the model domain. Water surface elevation was specified using harmonic constants of data recorded at this location by NOAA. At the boundary, salinity of 33 ppt was specified and the initial salinity in the model domain was also 33 ppt with a quiescent free surface and velocity field.

The vertical grid spacing was 0.2 m and the horizontal grid spacing was 200 m. Hydrodynamics and transport calculations were made for 377 639 active grid points and 12 442 active water columns. A time step of 60 s was chosen to comply with the stability condition on explicit horizontal advection. A 4-day simulation (5760 time steps) was run on a 200 MHz workstation in 47 h of CPU time.

In this simulation, the model was stable and the transport results allowed significant stratification to evolve. Figure 13, shows the horizontal variation of scalar concentration after 3.5 days of movement with the M_2 tide, while Figure 14 shows the vertical variation.

The maximum vertical Courant number during the simulation was $|c_z| = 5.2$ for a full cell. The total computational cost of a TRIM-3D simulation is roughly proportional to the number

© 1998 John Wiley & Sons, Ltd.

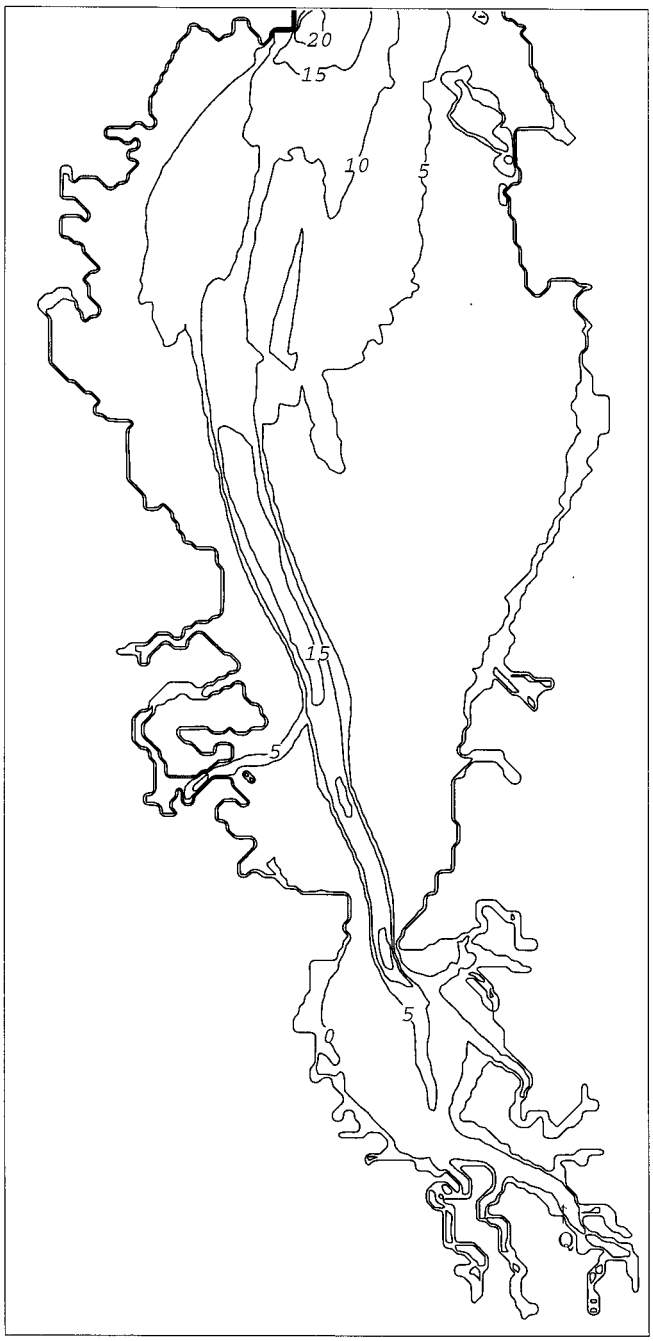

Figure 12. Model grid for SSFB with contours of depth in meters with Q indicating the location of freshwater discharge.

© 1998 John Wiley & Sons, Ltd.

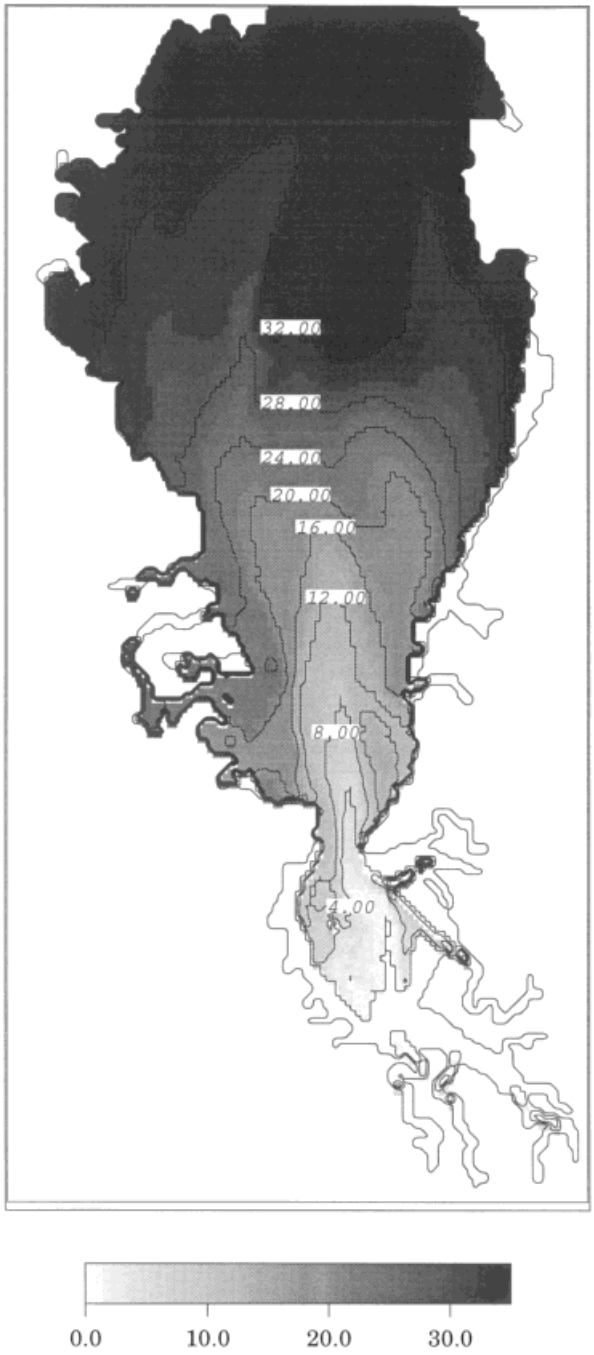

Figure 13. Horizontal salinity field 1 m below mean sea level in South San Francisco Bay after 3.5 days of freshwater discharge.

© 1998 John Wiley & Sons, Ltd.

of time steps in the simulation. The computation of vertical scalar advection required only 3.6% of the total computational time in the simulation. Thus the computational cost of the TRIM-3D model using the β method for vertical advection was $\approx 20\%$ of the computational cost if a time step limitation $c_z \leq 1$ were imposed by explicit conservative vertical transport.

Although TRIM-3D using the proposed method for vertical advection is much more efficient for this application than using an explicit conservative scheme for vertical advection, it is approximately twice as computationally expensive than using the non-conservative Eulerian–Lagrangian method. The proposed scheme is more expensive because there is a restriction on the horizontal Courant number imposed by the explicit, conservative horizontal advection scheme. In simulations of salinity using the Eulerian–Lagrangian method the time step could be increased roughly by a factor of two but cannot be increased further without violation of the baroclinic stability condition given by Equation (63).

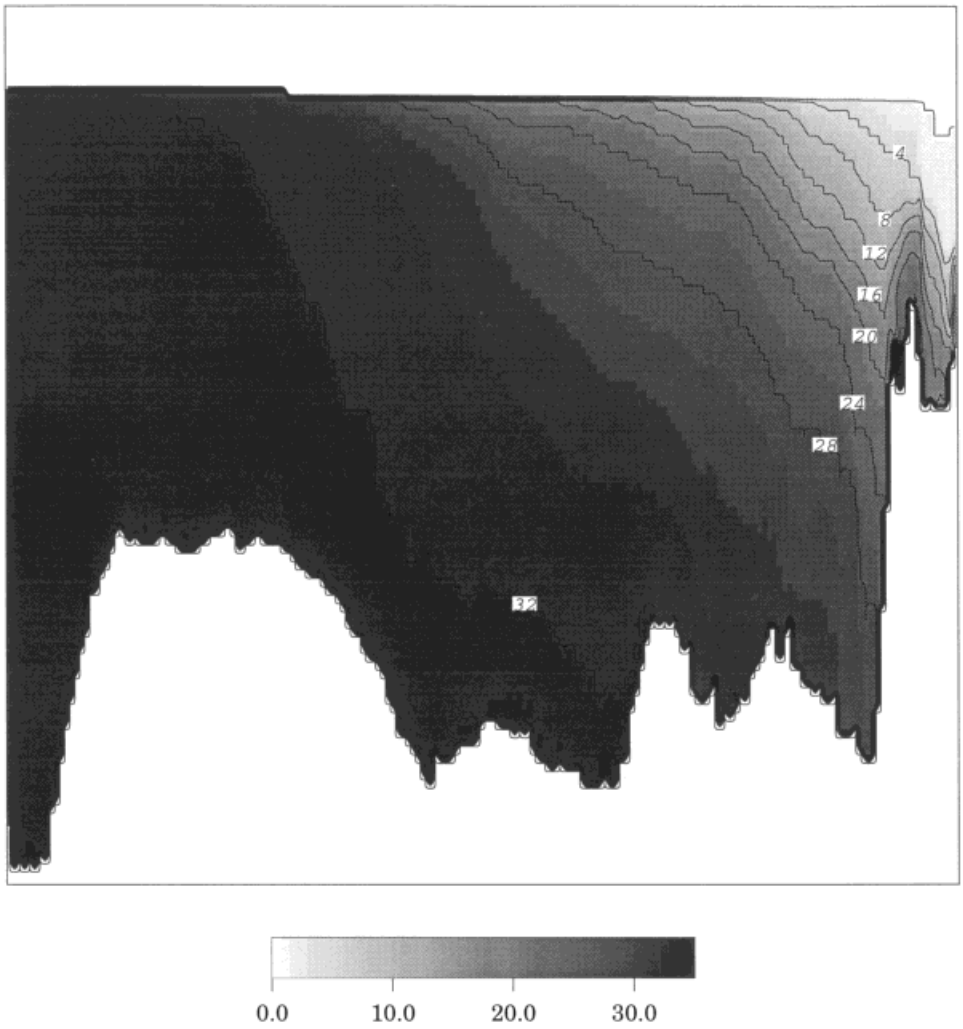

Figure 14. Vertical salinity distribution in the main channel of South San Francisco Bay after 3.5 days of freshwater discharge.

© 1998 John Wiley & Sons, Ltd.

In 74% of the transport calculations β was zero, so that no vertical numerical diffusion was introduced for these calculations. The average β value used for the transport calculations was $\beta = 0.0026$, which corresponds to a numerical diffusion coefficient of $\epsilon_{\text{num}} = 0.0097$ cm^2 s^{-1}. An estimate of the physical diffusion coefficient for vertical mixing in a well-mixed estuary is

$$\epsilon_{\text{phy}} = 0.0025 d U_a \tag{67}$$

where ϵ_{phy} is the eddy diffusivity, d is the local depth, and U_a is the velocity at mid-depth [19]. Typical values in SSFB range from $d = 1$ m, $U_a = 0.1$ m s^{-1}, $\epsilon_{\text{phy}} = 2.5$ cm^2 s^{-1} for the shoals and $d = 10$ m, $U_a = 1.0$ m s^{-1}, $\epsilon_{\text{phy}} = 250$ cm^2 s^{-1} for the channels. Thus, the numerical diffusion associated with the β method in this application is much smaller than estimates of physical diffusion in SSFB.

8. CONCLUSIONS

A one-dimensional, unconditionally stable semi-implicit method for the advection–diffusion equation has been outlined, and is useful in simulations where a large range of Courant numbers are present, but with high Courant numbers arising much less frequently than low Courant numbers. The scheme is more accurate than simpler implicit schemes, such as trapezoidal central differencing or trapezoidal upwind differencing, while maintaining unconditional stability and a tridiagonal matrix structure.

In multiple dimensions, the semi-implicit transport method can be used in one co-ordinate direction while an explicit transport scheme is used in the other co-ordinate directions. Because this approach allows a large time step to be used, it results in large computational savings compared with explicit conservative treatment of the vertical advection. The method is computationally more expensive than the non-conservative Eulerian–Lagrangian method, previously used with TRIM-3D [2], but guarantees scalar conservation and retains sharper vertical scalar gradients.

The simulation of salinity in South San Francisco Bay shows that the β method is stable and adequately efficient, even with high vertical resolution, for simulations of transport in estuaries over several tidal cycles. In addition, the numerical diffusion associated with this method was small, significant oscillations were not observed and the time step chosen was five times larger than it would have been for an explicit conservative method with a Courant number limitation $|c_z| < 1$.

ACKNOWLEDGMENTS

The research was conducted at CIRM (Centro Internazionale per la Ricerca Matematica), Trento, and the University of Trento, Italy. The first author was funded by the California Regional Water Quality Control 21 Boards (San Francisco Region) contract number 1-165-250-0 and the Leavell Family Faculty Scholarship.

REFERENCES

1. V. Casulli and E. Cattarli, 'Stability, accuracy and efficiency of a semi-implicit method for three-dimensional shallow water flow', *Comput. Math. Appl.*, **27**, 99–112 (1994).
2. V. Casulli and R.T. Cheng, 'Semi-implicit finite difference methods for three-dimensional shallow water flow', *Int. j. numer. methods fluids*, **15**, 629–648 (1992).

© 1998 John Wiley & Sons, Ltd.

3. C. Hirsch, *Numerical Computation of Internal and External Flows*, *Volume 1*, *Fundamentals of Numerical Discretization*, Wiley, New York, 1988.
4. B.P. Leonard, 'A stable and accurate convective modeling procedure based on quadratic upstream interpolation', *Comput. Meth. Appl. Mech. Eng.*, **19**, 59–98 (1979).
5. C. Hirsch, *Numerical Computation of Internal and External Flows*, *Vol. 2*, *Computational Methods for Inviscid and Viscous Flows*, Wiley, New York, 1990.
6. P.L. Roe, 'Some contributions to the modelling of discontinuous flows', *Lectures Appl. Math.*, **22**, 163–193 (1985).
7. I.D. James, 'Advection schemes for shelf sea models', *J. Mar. Sys.*, **8**, 237–254 (1996).
8. H.C. Yee, 'Construction of explicit and implicit symmetric TVD schemes and their applications', *J. Comput. Phys.*, **68**, 151–179 (1987).
9. R.A. Nunez Vaz and J.H. Simpson, 'Turbulence closure modeling of estuarine stratification', *J. Geophys. Res.*, **99(C)**, 16, 143–16, 160 (1994).
10. A.F. Blumberg and G.L. Mellor, 'A description of a three-dimensional coastal ocean circulation model', in N.S. Heaps (ed.), *Three-Dimensional Coastal Ocean Models*, *Coastal and Estuarine Sciences 4*, AGU, Washington, DC, 1987, pp. 1–16.
11. C.B. Vreugdenhil, 'Linear central finite difference methods', in C.B. Vreugdenhil and B. Korenm (eds.), Numerical Methods for Advection–Diffusion Problems, *Notes on Numerical Fluid Mechanics*, **45**, 27–54 (1993).
12. B.P. Leonard, 'The ULTIMATE conservative difference scheme applied to unsteady one-dimensional advection', *Comput. Methods Appl. Mech. Eng.*, **88**, 17–74 (1991).
13. V. Casulli, 'Semi-implicit finite difference methods for the two-dimensional shallow water equations', *J. Comput. Phys.*, **86**, 56–74 (1990).
14. E.S. Gross, Modeling scalar transport in a shallow estuary, *Ph.D. Dissertation* (in preparation), Stanford University, 1997.
15. A.E. Gill, *Atmosphere–Ocean Dynamics*, Academic Press, San Diego, 1982.
16. J.C.H. van Eijkeren, B.J. de Haan, G.S. Stelling and Th.L. van Stijn, 'Linear upwind biased methods', in C.B. Vreugdenhil and B. Korenm (eds.), Numerical Methods for Advection–Diffusion Problems, *Notes on Numerical Fluid Mechanics*, **45**, 55–91 (1993).
17. T.J. Conomos, R.E. Smith and J.W. Gartner, 'Environmental setting of San Francisco Bay', *Hydrobiology*, **129**, 1–12 (1985).
18. R.T. Cheng, V. Casulli and J.W. Gartner, 'Tidal, residual, intertidal mudflat (TRIM) model and its applications to San Francisco Bay, California', *Estuarine*, *Coastal*, *Shelf Sci.*, **36**, 235–280 (1993).
19. H.D. Fischer, E.J. List, R.C.Y. Koh, J. Imberger and N.H. Brooks, *Mixing in Inland and Coastal Waters*, Academic Press, San Diego, 1979.

© 1998 John Wiley & Sons, Ltd.